Bending/shear wave dispersion analysis of granular chains – Discrete and enriched continuous Cosserat modelling

Sina Massoumi, Noël Challamel, Jean Lerbet

Version of Record: https://www.sciencedirect.com/science/article/pii/S0020768321004285
Manuscript_a1c6937334bddae511c488d48e206a74

Bending/Shear Wave Dispersion Analysis of Granular Chains – Discrete and Enriched Continuous Cosserat Modelling

Sina Massoumi [a), 1], Noël Challamel [b), 2] and Jean Lerbet [a), 3]

[a)] *Univ. Evry – Université Paris-Saclay, Laboratoire de Mathématiques et Modélisation d'Evry, LaMME–UMR CNRS 8071, 23 bvd de France, 91037 Evry – France*

[b)] *Univ. Bretagne Sud, IRDL – UBS – UMR CNRS 6027, Centre de Recherche, Rue de Saint Maudé – BP 92116, 56321 Lorient cedex – France*

The current study focuses on the wave dispersion analysis of granular systems by investigating a paradigmatic one-dimensional discrete chain. Most of the analysis of the discrete problem are based on the discrete granular chain without additional confinement. This work is motivated by the detection of standing waves and negative velocity of acoustic and optical waves observed in discrete granular models. This study allows to understand better the incorporation between the theoretical models, granular materials and the included effective parameters. Concerning wave propagation, granular elements create a structured wave-guide network through which mechanical energy is transferred. In the presence of internal (microstructural) length scales, the elastic wave propagation problem involves an interplay between wave dispersion and structural features. The unidimensional granular chain is composed of uniform spherical grains elastically connected with both shear and rotational springs. The presented structural system can be considered as an elastic lattice model or a Cosserat chain model with shear interaction. We show how the elastic foundation

[1] E-mail : sina.massoumi@etud.univ-evry.fr
[2] E-mail : noel.challamel@univ-ubs.fr
[3] E-mail : jean.lerbet@univ-evry.fr.

affects the wave dispersion response of the system. The length scale (grain diameter) at which the system is probed, is an important issue bridging together multi-scale behavior and heterogeneity. In a first step, the wave dispersion of the discrete system is derived from the uncoupled mixed differential-difference equation of deflection. We further show that for infinite number of grains the dispersion equation of the discrete model converges toward the continuum model of Bresse-Timoshenko. The wave dispersive properties of this discrete model are investigated also in the Brillouin zone. Next, the discrete to continuous model is approximated by the methods of Taylor polynomial development and Padé rational expansion. Finally, a comprehensive dispersive analysis is done through the dispersion equations of the discrete model, the discrete to continuous approximation beam and the continuous one. Some experimental results for Carbon Nanotubes (CNTs) are replicated by the model. We show that the model is able to predict accurately the positive and negative group of wave velocity as well as the standing wave. Scale effects and wave dispersive characteristics of the granular chain are captured by the continuous gradient elasticity model.

Keywords: Granular chain; Dispersion analysis; Lattice formulation; Enriched continua; Wave propagation ; Nonlocal beams ; Scale effect ; Cosserat modelling ; Shear effects ; Gradient elasticity

1. Introduction

The wave propagation characteristics of conventional forms of matter are well understood and well documented. In contrast, waves in granular media are more complex due to the discrete nature of these system, which may include nonlinear interactions. Considerable interest in the dynamic response of granular media exists in the geomechanics community typically involving acoustics and wave propagation in sand, gravel and rock materials. Granular materials which can be modelled by both discrete and continuous approaches, are involved in many engineering applications such as biomedical engineering, mechanical engineering, food engineering or civil engineering. Mechanical energy is transferred through a structured wave-guide network which is created by granular media. The key element in the mechanics of a granular system is the force chain. It is along these preferentially stressed chains of particles that waves are transmitted. These nonlinear chains are heavily dependent on the geometry of the bed and are prone to rearrangement even by the slightest of forces.

In presence of length scales, the elastic wave propagation problem involves an interplay between wave dispersion and structural features. Dispersion is a real issue in wave propagation since each granular element acts as a filter for the frequencies (letting the low frequencies or large wave-lengths pass through). In addition to dispersion, the material can delay or block the high frequencies (short wavelengths).

Classical elasticity theories are not suitable for capturing the wave dispersion in granular materials when the microstructured influence is predominant in the wave propagation. For these cases, the long-range interactions are important to take into account in the deformation process (for instance the book of Bagdoev et al. [1] or Vardoulakis [2]). Unlike local elasticity formulations, higher order

continuum theories (Mindlin [3] and Aifantis [4]) and non-local theories (Eringen [5]) describe the dispersive behavior more accurately by considering some scale effects induced by the granular microstructure.

The advantage of discrete models in comparison with the continuum ones is their ability to describe better the inhomogeneous effects at the particle level. In recent decades, several models have been developed on the granular chains in order to understand deeper the static and dynamic behavior of these structures and predict more precisely the wave dispersion. Microstructural models of granular media based on both translation and rotational degrees of freedom have been initially investigated for regular granular packing by Duffy [6] and for random granular packing by Digby [7] and Chang [8]. Mühlhaus and Vardoulakis [9] analyzed the influence of additional degrees of freedom on the familiar translational motion (see also La-Valle and Massoumi [10]). This has led to formulations of the micro-polar type or Cosserat-type theories for random packing of granulates (Suiker et al. [11]). Chang and Ma [12] studied the random packing of grains based on linear elastic contact interactions with the isotropic distribution. Using the same concept for static analysis, the buckling behavior of the granular chain has recently been investigated by Challamel et al. [13]. Schwartz et al. [14] studied the vibrational behavior of solid grains by having particle rotation and translation together (Cosserat discrete model) while assuming only shear elastic interaction for both ordered and disordered packings. Gomez-Silva and Zaera [15] modelled a Hencky beam model (discrete flexural media) assuming only bending interactions. The model of Schwartz et al. [13] has been generalized using a discrete Cosserat model with the consideration of both shear and rotation interactions (Pasternak and Mühlhaus [16], Pichard et al. [17],Vasiliev et al. [18] and Massoumi et al. [19] for instance). In particular, Pasternak and Mühlhaus [16] and

Pichard et al. [17] obtained the wave dispersive behavior in a one dimensional discrete granular chain with linearly elastic shear and rotation interactions.

Due to the importance of dynamic properties and functions of one-dimensional granular media, several studies have been done in various domains. Toward this aim, studying the phenomena involved using simple analytical models is beneficial. Starosvetsky et al. [20] studied the dynamic behavior of nonlinear granular chains with Hertz interaction. The problem of nonlinear perturbations in one-dimensional granular chain is investigated by Nesterenko [21] in Hertzian contact. Herbold et al. [22] analyzed the formation and propagation of nonstationary signals in linear and nonlinear diatomic periodic one-dimensional granular chains. The free vibration of a granular chain with both bending and shear granular interactions rested on simply supported boundary conditions and elastic foundations is studied by Massoumi et al. [23]. In the present paper, the same discrete Cosserat model with both rotation and shear elastic interactions will be considered, which could be understood as an equivalent discrete Bresse-Timoshenko model (Bresse [24] and Timoshenko [25, [26]- see also Challamel and Elishakoff [27]).

The current study focuses on the analysis of wave propagation and the dispersive behavior of mechanical waves in a discrete granular media resting on elastic foundations. Misra and Nejadsadeghi [28] studied the dispersive behavior of granular materials in response to elastic deformation waves using granular micromechanics approach proposed by Misra and Poorsolhjouy [29]. This paper can be considered also as the discrete study of the continuous Bresse-Timoshenko beam on continuous linear elastic foundation (Winkler foundation). Assuming an infinite number of grains, the results lead to the response of a continuous Bresse-Timoshenko beam on elastic foundation, studied for instance by Wang and Stephens [30], Cheng and Pantelides [31] or Manevich [32]. In particular, the dispersive behavior of continuous Bresse-Timoshenko beam resting on elastic foundation has been specifically addressed by Manevich [32]. The Bresse-

Timoshenko continuum limit may be also understood as the long wave limit of the discrete granular model. The granular chain composed of rigid grains is assumed to interact with a Winkler elastic foundation (Winkler [33]). The wave dispersion of this granular system is derived from the uncoupled equation of motion using a discrete Cosserat theory, based on both rotational and translational degrees of freedom for each grain. For the long wave limit, the dispersion equation converges towards the continuum model of Bresse-Timoshenko beam on Winkler foundation, as treated by Manevich [20]. Also, the results valid for the discrete granular beam could be well compared to the ones of Pasternak and Mühlhaus [16] and Pichard et al. [17], neglecting the foundation contribution (k=0). Next, the nonlocal dispersion results are obtained through the homogenization of the fourth-order difference equation of the system by applying Taylor series and Padé approximation. Finally, a comparison between the discrete and the enriched continuous model will be discussed and conclusions sections are presented. A comprehensive dispersion analysis is done regarding the local and nonlocal deflection equations of this 1D granular chain. Based on the presented parametric study, the wave dispersion curves for the discrete lattice models are compared to the corresponding continuum models (Bresse-Timoshenko). The results also compared to molecular dynamics of the flexural behavior in carbon nanotubes with acceptable coincidence. The results of this paper generalize the ones of Pasternak and Mühlhaus [16] and Pichard et al. [17] valid for the wave propagation of elastic chain without elastic foundation. Understanding the wave propagation in one-dimensional systems is useful if one better wants to analyze the complex wave propagation phenomena in two-dimensional and three-dimensional granular systems (both in the elastic and the inelastic ranges).

2. Granular Model

A 1D granular chain (or granular beam) composed of spherical uniform rigid grain with diameter a resting on an elastic foundation is considered. These rigid grains are connected elastically by shear and rotational springs as shown in Fig. 1. Each grain has two degrees of freedom which are represented by w_i and θ_i for grain number i. Such a force chain allows us to illustrate the heterogeneous nature of granular media. The length scale (grain diameter) at which the system is probed is an important issue bridging together multi-scale behavior and heterogeneity.

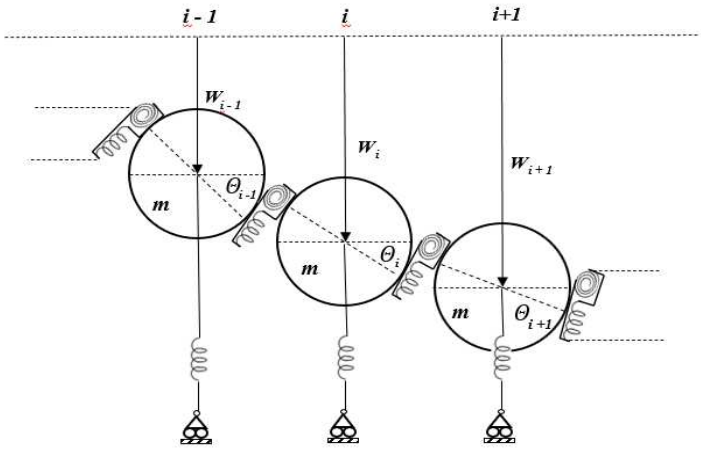

Fig. 1. A discrete shear granular chain composed of grains with diameter a and mass m

The bending/shear wave propagation equation is a system of governing mixed functional differential equation (or mixed differential-difference equation - see Myshkis [34] for the general investigation of mixed differential-difference equations). Studying the equilibrium of force and moment (second-newton laws) of such a system for each grain leads to the following equations system

$$\begin{aligned} \boldsymbol{V}_{i+\frac{1}{2}} - \boldsymbol{V}_{i-\frac{1}{2}} - \boldsymbol{F}_i &= \boldsymbol{m}\ddot{\boldsymbol{w}}_i, \\ \boldsymbol{M}_{i+1/2} - \boldsymbol{M}_{i-\frac{1}{2}} + \frac{\boldsymbol{a}}{2}(\boldsymbol{V}_{i+\frac{1}{2}} + \boldsymbol{V}_{i-\frac{1}{2}}) &= \boldsymbol{I}_m\ddot{\boldsymbol{\Theta}}_i \end{aligned} \tag{1}$$

where the shear, bending and elastic foundation terms defined as follows

$$M_{i+\frac{1}{2}} = C(\theta_{i+1} - \theta_i), \qquad V_{i+\frac{1}{2}} = S\left(W_{i+1} - W_i - \frac{a}{2}(\theta_{i+1} + \theta_i)\right),$$

$$M_{i-\frac{1}{2}} = C(\theta_i - \theta_{i-1}), \qquad V_{i-\frac{1}{2}} = S\left(W_i - W_{i-1} - \frac{a}{2}(\theta_i + \theta_{i-1})\right), \tag{2}$$

$$F_i = kaw_i$$

Substituting Eq. (2) in Eq. (1) leads to

$$S(w_{i+1} + w_{i-1} - 2w_i) - \frac{a}{2}S(\theta_{i+1} - \theta_{i-1}) - kaw_i - m\ddot{w}_i = 0,$$
$$C(\theta_{i+1} + \theta_{i-1} - 2\theta_i) + \frac{a}{2}S(w_{i+1} - w_{i-1}) - \frac{a^2}{4}S(\theta_{i+1} + \theta_{i-1} + 2\theta_i) - I_m\ddot{\theta}_i = 0 \tag{3}$$

where S is the shear stiffness defined as $S = \frac{K_S GA}{a}$ in which G is the shear modulus, A is the cross-sectional area and K_s is the shear correction coefficient. C is the rotational stiffness defined as $C = \frac{EI}{a}$, E is Young's modulus and I is the second moment of area. I_m is the second moment of inertia for the grain ($I_m = \rho Ia$), $m = \rho a$ and K=ka is the discrete stiffness of the elastic support that is located in the center of each grain.

Eq. (3) has been obtained by Pasternak and Mühlhaus [16], Pichard et al. [17] and Vasiliev et al. [18] omitting Winkler elastic foundations. Also neglecting the rotational interactions ($C = 0$) and the Winkler elastic foundations ($k = 0$) in Eq. (3) leads to the equilibrium equations of Schwartz et al. [14].

The difference operators of δ_0, δ_1 and δ_2 are introduced as follows**:**

$$\delta_0 w = \frac{w_{i+1} + 2w_i + w_{i-1}}{4}, \qquad \delta_1 w = \frac{w_{i+1} - w_{i-1}}{2a}, \qquad \delta_2 w = \frac{w_{i+1} - 2w_i + w_{i-1}}{a^2} \tag{4}$$

The following relations could be expressed between these operators.

$$\delta_2\delta_0 = \delta_0\delta_2 = {\delta_1}^2 \tag{5}$$

The equation of motion expressed by the transverse deflection governed to the model is a linear fourth-order difference equation in space. Using the properties of the difference operators in Eq. (5), the dynamic equation for the deflection of the granular chain (granular lattice model) is obtained as

$$[EI\delta_2{}^2 - \left(\rho I\partial_t{}^2 + \frac{kEI}{K_sGA} + \frac{EI\rho\partial_t{}^2}{K_sG}\right)\delta_2 + (k + \rho A\partial_t{}^2)\delta_0 + \frac{k\rho I\partial_t{}^2}{K_sGA} + \frac{\rho^2 I\partial_t{}^4}{K_sG}]w_i = 0 \tag{6}$$

This difference equation obtained by Massoumi et al. [23] also leads to the equation obtained by Pasternak and Mühlhaus [16] with ignorance of the Winkler elastic foundations. Eq. (6) could be simplified for the static range (Challamel et al. [13]) as follows

$$[EI\delta_2{}^2 - \left(\frac{kEI}{K_sGA}\right)\delta_2 + k\delta_0]w_i = 0 \tag{7}$$

Neglecting the Winkler elastic foundation in Eq. (6) leads to

$$[\delta_2{}^2 - \partial_t{}^2\left(\frac{\rho}{E} + \frac{\rho}{K_sG}\right)\delta_2 + \partial_t{}^2(\frac{\rho A}{EI}\delta_0 + \frac{\rho^2\partial_t{}^2}{EK_sG})]w_i = 0 \tag{8}$$

This model is slightly different from the granular model studied by Duan et al. [35]. Duan et al. [35] studied the dynamic analysis of a discrete beam in bending with shear interactions consisted of rigid links where the displacement fields are defined at the joint element. The difference equation of that model could be represented as follows

$$\left[\delta_2{}^2 - \partial_t{}^2\left(\frac{\rho}{E} + \frac{\rho}{K_sG}\right)\delta_2 + \partial_t{}^2\left(\frac{\rho A}{EI} + \frac{\rho^2\partial_t{}^2}{EK_sG}\right)\right]w_i = 0 \tag{9}$$

The origin of the difference comes from the appearance of the pseudo-difference operator δ_0 that stems from the enhanced shear interaction modeling of the granular elements.

For the continuous beam model assuming an infinite number of grains ($n \to \infty$), Eq. (6) converges to the fourth-order differential equation of Eq. (10) (continuum local) which is valid for a Bresse-Timoshenko beam in the absence of Winkler foundations ($k = 0$).

$$\left[\partial_x^4 - \left(\frac{\rho\partial_t{}^2}{E}\left(1 + \frac{E}{K_s G}\right) + \frac{k}{K_s GA}\right)\partial_x^2 + \left(\frac{\rho\partial_t{}^2}{E}\left(\frac{A}{I} + \frac{k}{K_s GA} + \frac{\rho\partial_t{}^2}{K_s G}\right) + \frac{k}{EI}\right)\right] w = 0 \tag{10}$$

The aforementioned differential equation has been obtained by Wang and Stephens [30], Cheng and Pantelides [31] and Manevich [32].

3. Wave Dispersion Analysis

3.1. Discrete Approach via Exact Solution

Dispersion of propagation waves would influence the media if the wavelength is of the same magnitude order as the characteristic spacing of the dominant source of heterogeneity. In order to capture wave dispersion, continuum models need to be equipped with appreciate terms that capture the lower scale behavior (Domenico and Askes [36]).

To satisfy the fourth-order differential equation of Eq. (6) (granular lattice model), a fundamental solution in the harmonic form could be considered as follow:

$$w_i = \beta e^{j(\omega t - k_w x_i)} \tag{11}$$

Substitution of the expression Eq. (11) into Eq. (6) provides the algebraic equation as:

$$\beta e^{j(\omega t - k_w x_i)}[\left(e^{2ak_w j} - 4e^{ak_w j} + 6 - 4e^{-ak_w j} + e^{-2ak_w j}\right) + a^2\left(\frac{\rho\omega^2}{E} - \frac{k}{K_s GA} + \frac{\rho\omega^2}{K_s G}\right)\left(e^{ak_w j} - 2 + e^{-ak_w j}\right) + a^4\left(\frac{k}{4EI} - \frac{\rho A\omega^2}{4EI}\right)\left(e^{ak_w j} + 2 + e^{-ak_w j}\right) + a^4\left(-\frac{k\rho\omega^2}{EK_s GA} + \frac{\rho^2\omega^4}{EK_s G}\right)] = 0 \tag{12}$$

The following biquadratic equation expressed by the angular frequency could be obtained from Eq. (12):

$$[\rho a^2]\omega^4 - 4\left[(K_sG + E)\,sin^2\left(\frac{ak_w}{2}\right) + \frac{Aa^2K_sG}{4I}cos^2\left(\frac{ak_w}{2}\right) + \frac{ka^2}{4A}\right]\omega^2 + \left[16\frac{EK_sG}{\rho a^2}sin^4\left(\frac{ak_w}{2}\right) + k\left(\frac{4E}{\rho A}sin^2\left(\frac{ak_w}{2}\right) + \frac{a^2K_sG}{\rho I}cos^2\left(\frac{ak_w}{2}\right)\right)\right] = 0 \quad (13)$$

Neglecting the Winkler foundation ($k = 0$), the aforementioned equation leads to the results obtained by Pasternak and Mühlhaus [16] (Eq. (14)).

$$[MN]\omega^4 - 4\left[(NS + MC)\,sin^2\left(\frac{ak_w}{2}\right) + \frac{MSa^2}{4}cos^2\left(\frac{ak_w}{2}\right)\right]\omega^2 + \left[16SC\,sin^4\left(\frac{ak_w}{2}\right)\right] = 0 \quad (14)$$

with $M = \rho Aa$ and $N = I_m = \rho Ia$. Two asymptotic cases for a granular chain could be obtained from Eq. (13) supposing pure shear and or pure bending. Assuming only shear interaction ($E = 0$)

$$[\rho a^2]\omega^4 - 4\left[K_sG\,sin^2\left(\frac{ak_w}{2}\right) + \frac{Aa^2K_sG}{4I}cos^2\left(\frac{ak_w}{2}\right) + \frac{ka^2}{4A}\right]\omega^2 + \left[\frac{a^2K_sGk}{\rho I}cos^2\left(\frac{ak_w}{2}\right)\right] = 0 \quad (15)$$

This equation leads to the following quadratic equation of Schwartz et al. [14] with respect to the angular frequency by omitting Winkler foundation ($k = 0$):

$$\left[\omega^2 - \omega_0^2\left(sin^2\left(\frac{ak_w}{2}\right) + \alpha\,cos^2\left(\frac{ak_w}{2}\right)\right)\right]\omega^2 = 0 \quad (16)$$

in which $\omega_0^2 = \frac{4S}{M}$ and $\alpha = \frac{Mr^2}{I_m}$. On the other hand, considering only the rotational effect ($G = 0$) in Eq. (13) leads to

$$[\rho a^2]\omega^4 - 4\left[E\,sin^2\left(\frac{ak_w}{2}\right) + \frac{ka^2}{4A}\right]\omega^2 + \left[\frac{4Ek}{\rho A}sin^2\left(\frac{ak_w}{2}\right)\right] = 0 \quad (17)$$

For the continuum case by assuming an infinite number of grains Eq. (13) leads to the quartic equation obtained by Manevich [32] as follows

$$[\mathcal{X}]\varpi^4 - [1 + (1 + \mathcal{X})\hbar^2 + w_1\mathcal{X}]\varpi^2 + [w_1(1 + \mathcal{X}\hbar^2) + \hbar^4] = 0 \quad (18)$$

in which $w_1 = \frac{I}{EA^2}k$, $\mathcal{X} = \frac{E}{K_S G}$, $\varpi^2 = \frac{I\rho}{EA}\omega^2$ and $\mathcal{k}^2 = \frac{I}{A}{k_w}^2$. Introducing the non-dimensional quantities as follows:

$$\boldsymbol{\Omega_{b,s}} = \frac{\boldsymbol{a}}{\boldsymbol{c_{b,s}}}\boldsymbol{\omega} \ , \ \boldsymbol{\mu_s} = \frac{\boldsymbol{E}}{\boldsymbol{K_s\, G}} \ , \boldsymbol{r^*} = \frac{\boldsymbol{1}}{\boldsymbol{a}}\sqrt{\frac{\boldsymbol{I}}{\boldsymbol{A}}} \ , \ \ \boldsymbol{k^*} = \frac{\boldsymbol{ka^4}}{\boldsymbol{EI}} \tag{19}$$

where c_0 is the one-dimensional wave velocity and could be defined by either shear or bending beam parameters as $c_{bending} = \sqrt{\frac{EI}{\rho A a^2}}$ and $c_{shear} = \sqrt{\frac{K_s G}{\rho}}$. Eq. (13) could be rewritten in the following form

$$\begin{aligned}\boldsymbol{\Omega_b}^4 - \left[\left(\frac{\boldsymbol{4}}{\boldsymbol{\mu_s r^{*2}}} + \frac{\boldsymbol{4}}{\boldsymbol{r^{*2}}}\right)\boldsymbol{sin^2}\left(\frac{\boldsymbol{ak_w}}{\boldsymbol{2}}\right) + \frac{\boldsymbol{1}}{\boldsymbol{\mu_s r^{*4}}}\boldsymbol{cos^2}\left(\frac{\boldsymbol{ak_w}}{\boldsymbol{2}}\right) + \boldsymbol{k^*}\right]\boldsymbol{\Omega_b}^2 \\ + \left[\boldsymbol{16}\frac{\boldsymbol{1}}{\boldsymbol{\mu_s r^{*4}}}\boldsymbol{sin^4}\left(\frac{\boldsymbol{ak_w}}{\boldsymbol{2}}\right) + \boldsymbol{k^*}\left(\frac{\boldsymbol{4}}{\boldsymbol{r^{*2}}}\boldsymbol{sin^2}\left(\frac{\boldsymbol{ak_w}}{\boldsymbol{2}}\right) + \frac{\boldsymbol{1}}{\boldsymbol{\mu_s r^{*4}}}\boldsymbol{cos^2}\left(\frac{\boldsymbol{ak_w}}{\boldsymbol{2}}\right)\right)\right] = \boldsymbol{0}\end{aligned} \tag{20}$$

or through the shear wave velocity definition

$$\begin{aligned}\boldsymbol{\Omega_s}^4 - \left[(\boldsymbol{4} + \boldsymbol{4\mu_s})\,\boldsymbol{sin^2}\left(\frac{\boldsymbol{ak_w}}{\boldsymbol{2}}\right) + \frac{\boldsymbol{1}}{\boldsymbol{r^{*2}}}\boldsymbol{cos^2}\left(\frac{\boldsymbol{ak_w}}{\boldsymbol{2}}\right) + \boldsymbol{k^*\mu_s r^{*2}}\right]\boldsymbol{\Omega_s}^2 \\ + \left[\boldsymbol{16\,\mu_s sin^4}\left(\frac{\boldsymbol{ak_w}}{\boldsymbol{2}}\right) + \boldsymbol{k^*\mu_s}\left(\boldsymbol{4\mu_s r^{*2}}\,\boldsymbol{sin^2}\left(\frac{\boldsymbol{ak_w}}{\boldsymbol{2}}\right) + \boldsymbol{cos^2}\left(\frac{\boldsymbol{ak_w}}{\boldsymbol{2}}\right)\right)\right] = \boldsymbol{0}\end{aligned} \tag{21}$$

In order to know the nature of the results for Eq. (13), the sign of the coefficients in the characteristic equation need to be clarified.

$\forall\, \boldsymbol{E, G, k, I, A, K_s, a, k_w}$:

$$\boldsymbol{\rho a^2 > 0},$$

$$\boldsymbol{-4\left((K_s G + E)\,sin^2\left(\frac{ak_w}{2}\right) + \frac{Aa^2 K_s G}{4I}cos^2\left(\frac{ak_w}{2}\right) + \frac{ka^2}{4A}\right) < 0},$$

$$\boldsymbol{16\frac{EK_s G}{\rho a^2}sin^4\left(\frac{ak_w}{2}\right) + k\left(\frac{4E}{\rho A}sin^2\left(\frac{ak_w}{2}\right) + \frac{a^2 K_s G}{\rho I}cos^2\left(\frac{ak_w}{2}\right)\right) > 0} \tag{22}$$

The discriminant (Δ) of Eq. (13) would be obtained as follows

$$\Delta_1 = \left[(K_sG - E)\,sin^2\left(\frac{ak_w}{2}\right)\right]^2 + \left[\frac{Aa^2K_sG}{4I}cos^2\left(\frac{ak_w}{2}\right) - \frac{ka^2}{4A}\right]^2 + \left[2E\,sin^2\left(\frac{ak_w}{2}\right)\right]\left[\frac{Aa^2K_sG}{4I}cos^2\left(\frac{ak_w}{2}\right) - \frac{ka^2}{4A}\right] + \left[2K_sG\,sin^2\left(\frac{ak_w}{2}\right)\right]\left[\frac{Aa^2K_sG}{4I}cos^2\left(\frac{ak_w}{2}\right) + \frac{ka^2}{4A}\right] \quad (23)$$

Considering Eq. (23) as a function of Winkler elastic foundation leads to the following parabolic equation

$$f(k) = \left(\left[\frac{a^2}{4A}\right]^2\right)k^2 - \left(\frac{a^4K_sG}{8I}cos^2\left(\frac{ak_w}{2}\right) + (E - K_sG)(\frac{a^2}{2A})\,sin^2\left(\frac{ak_w}{2}\right)\right)k + ((\frac{Aa^2K_sG}{4I}cos^2\left(\frac{ak_w}{2}\right))(\frac{Aa^2K_sG}{4I}cos^2\left(\frac{ak_w}{2}\right) + 2(E + K_sG)\,sin^2\left(\frac{ak_w}{2}\right)) + \left[(K_sG - E)\,sin^2\left(\frac{ak_w}{2}\right)\right]^2) \quad (24)$$

$f(0)$ leads to the result obtained by Pasternak and Mühlhaus [16]. Here an attempt is made to identify the effect of adding elastic foundation to the model, for the dynamic response of the system.

$\forall\, E, G, I, A, K_s, a, k_w$:

$$\left[\frac{a^2}{4A}\right]^2 > 0\,,\ \Delta_2 = -\frac{(a^3K_sG)^2}{16AI}sin^2(ak_w) < 0 \quad (25)$$

It can be concluded that the parabolic equation of Eq. (24) is upward with the minimum positive value of $\frac{-4A^2\Delta_2}{a^4}$. On the other hand, the behavior of Eq. (23) depending on k_w is studied for any physical parameters of the system. All terms of the discriminant (Δ_1) are positive except the third one. Therefore, the discriminant of Eq. (13) (Δ_1) is always positive for any values of Winkler elastic foundation and mode number. This fact with regard to Eq. (22) leads to two real positive solutions for Eq. (13) expressed by natural frequency.

Here the nature of the wave is tried to be clarified. Substituting the exponential form of Eq. (11) for θ_i and w_i by $\theta_i = \alpha e^{j(\omega t - k_w x_i)}$ and $w_i = \beta e^{j(\omega t - k_w x_i)}$ in the equilibrium equation system of Eq. (3) while assuming $\omega = k_w v_p$, leads to:

$$\begin{aligned} -4\beta S \sin\left(\frac{ak_w}{2}\right)^2 - a\alpha Sj \sin(ak_w) - a\beta k + \beta m {k_w}^2 {v_p}^2 = 0, \\ -4\alpha C \sin\left(\frac{ak_w}{2}\right)^2 + a\beta Sj \sin(ak_w) - a^2 \alpha S \cos\left(\frac{ak_w}{2}\right)^2 - \alpha I_m {k_w}^2 {v_p}^2 = 0 \end{aligned} \tag{26}$$

in which v_p is the phase velocity. The dynamic response of this coupled system of equation can be obtained in the following form

$$\omega^2 = \frac{\sigma \pm \sqrt{\sigma^2 - 4\tau}}{2} \tag{27}$$

where σ and τ are represented by

$$\begin{aligned} \sigma &= \frac{4}{\rho a^2}(K_s G + E) sin^2\left(\frac{ak_w}{2}\right) + \frac{AK_s G}{\rho I} cos^2\left(\frac{ak_w}{2}\right) + \frac{k}{\rho A}, \\ \tau &= 16 \frac{EK_s G}{\rho^2 a^4} sin^4\left(\frac{ak_w}{2}\right) + \frac{k}{\rho a^2}\left(\frac{4E}{\rho A} sin^2\left(\frac{ak_w}{2}\right) + \frac{a^2 K_s G}{\rho I} cos^2\left(\frac{ak_w}{2}\right)\right) \end{aligned} \tag{28}$$

Regarding to the two positive responses of Eq. (27), the phase velocity could be obtained for $k_w \rightarrow 0$ as follows

$$v_p = \sqrt{\frac{\sigma \pm \sqrt{\sigma^2 - 4\tau}}{2{k_w}^2}} \xrightarrow{k_w \to 0} v_p \approx \sqrt{\frac{\left(\frac{AK_s G}{\rho I} + \frac{k}{\rho A}\right) \pm \left|\frac{AK_s G}{\rho I} - \frac{k}{\rho A}\right|}{2{k_w}^2}} \tag{29}$$

The ratio of the amplitudes (α/β) can be found from Eq. (26). The first relation leads to

$$\frac{\alpha}{\beta} = j \frac{4S \sin\left(\frac{ak_w}{2}\right)^2 + ak - m{k_w}^2 {v_p}^2}{aS \sin(ak_w)} \tag{30}$$

Supposing $k = 0$, Eq. (30) leads to the result obtained by Pasternak and Mühlhaus [16]. According to Eq. (29) and the positive root of Eq. (30) for the low value of mode number (long-wave limit), only the rotational wave could propagate in the system.

$$\boldsymbol{k_w \to 0}: \quad \frac{\alpha}{\beta} \approx j\frac{ak - \frac{aA^2K_sG}{I}}{aS\,sin(ak_w)} \approx \infty \text{ (Rotational wave)} \tag{31}$$

While regarding to the other branch (the negative root), the shear term of the wave appears as follows

$$\boldsymbol{k_w \to 0}: \quad \frac{\alpha}{\beta} \approx j\frac{2}{a}tan\left(\frac{ak_w}{2}\right) \approx 0 \text{ (Shear wave)} \tag{32}$$

The oscillations here are the displacement of the grains in directions perpendicular to the propagation of the wave. Therefore, with the foundation, the wave nature is mixed of both types that one is dominant to the other one and it can be considered as a shear-rotational wave. The mode number cannot exceed the grain number value or in the other words, the wave length cannot be shorter than the grain size. Thus, the assumption of $k_w \to \infty$ can be true only for an infinite number of grains or continuum beam.

On the other hand, by neglecting the Winkler foundation, the phase velocity for a small value of mode number leads to

$$v_{p1} = \sqrt{\frac{\sigma - \sqrt{\sigma^2 - 4\tau}}{2k_w^{\,2}}} \xrightarrow{k_w \to 0} v_p \propto k_w,$$

$$v_{p2} = \sqrt{\frac{\sigma + \sqrt{\sigma^2 - 4\tau}}{2k_w^{\,2}}} \xrightarrow{k_w \to 0} v_p \propto \frac{1}{k_w} \tag{33}$$

Using again the coefficient ratio of Eq. (30) for the long waves and $k = 0$ leads to the dominancy of the shear component when taking into account the first spectrum of the results of Eq. (32) as follows:

$$\boldsymbol{k_w \to 0}: \frac{\boldsymbol{\alpha}}{\boldsymbol{\beta}} \approx \mathbf{0} \quad \text{(Shear wave)} \tag{34}$$

While for the second spectrum or the higher frequency branch, the rotational wave is dominated to the system.

$$\boldsymbol{k_w \to 0}: \frac{\boldsymbol{\alpha}}{\boldsymbol{\beta}} \approx \infty \quad \text{(Rotational wave)} \tag{35}$$

Thus, without the Winkler elastic foundation, the wave nature is also combined of both types (Pasternak and Mühlhaus [16]).

On the other hand, the mixed differential-difference equation for a Hencky beam problem or discrete Euler-Bernoulli beam theory has been obtained as

$$\left[\boldsymbol{EI{\delta_2}^2 + \rho A{\partial_t}^2}\right]\boldsymbol{w_i} = \mathbf{0} \tag{36}$$

Regarding to the properties of Eq. (4), Eq. (36) leads to

$$\boldsymbol{EI}\left(\boldsymbol{e^{2ak_wj} - 4e^{ak_wj} + 6 - 4e^{-ak_wj} + e^{-2ak_wj}}\right) - \boldsymbol{\rho A a^4 \omega^2} = \mathbf{0} \tag{37}$$

This equation can be simplified as

$$\frac{\boldsymbol{I}}{\boldsymbol{a^4}}(\mathbf{2cos}(\boldsymbol{2ak_w}) - \mathbf{8\,cos}(\boldsymbol{ak_w}) + \mathbf{6}) - \frac{\boldsymbol{\rho A}}{\boldsymbol{E}}\boldsymbol{\omega^2} = \mathbf{0} \tag{38}$$

the quadratic wave dispersive equation would be obtained as follows in a dimensionless form with respect to the angular frequency of the granular chain with pure bending interactions:

$$\boldsymbol{{\Omega_b}^2} = \mathbf{16}\,\boldsymbol{sin^4}\left(\frac{\boldsymbol{ak_w}}{\mathbf{2}}\right) \tag{39}$$

This equation associated with the discrete granular chain may be efficiently approximated by a nonlocal equation associated with the wave propagation in a nonlocal continuous beam.

On the other hand, let's consider the case of a granular chain with predominant bending interactions ($S \to \infty$) and neglecting Winkler foundation ($k = 0$). In this case, the wave propagation equation expressed by transverse deflection for the granular system (Eq. (6)) leads to

$$[EI\delta_2{}^2 + \partial_t{}^2(\rho A\delta_0 - \rho I\delta_2)]w_i = 0 \tag{40}$$

This equation leads to the following relation by using the definitions of Eq. (4)

$$\beta e^{j(\omega t - k_w x_i)}[\left(e^{2ak_w j} - 4e^{ak_w j} + 6 - 4e^{-ak_w j} + e^{-2ak_w j}\right) + a^2\left(\frac{\rho\omega^2}{E}\right)\left(e^{ak_w j} - 2 + e^{-ak_w j}\right) + a^4\left(-\frac{\rho A\omega^2}{4EI}\right)\left(e^{ak_w j} + 2 + e^{-ak_w j}\right)] = 0 \tag{41}$$

Which can be simplified as

$$16\,sin^4\left(\frac{ak_w}{2}\right) + \frac{a^2}{A}\left(\frac{\rho A\omega^2}{E}\right)\left(4\,sin^2\left(\frac{ak_w}{2}\right)\right) - \frac{a^4}{I}\left(\frac{\rho A\omega^2}{E}\right)\left(cos^2\left(\frac{ak_w}{2}\right)\right) = 0 \tag{42}$$

Using Eq. (19) for the non-dimensional frequency with $c_{bending}$, one could be found as follows

$$\Omega_b{}^2 = \frac{16\,sin^4\left(\frac{ak_w}{2}\right)}{cos^2\left(\frac{ak_w}{2}\right) - 4r^{*2}\,sin^2\left(\frac{ak_w}{2}\right)} \tag{43}$$

Neglecting the rotational inertia terms leads to the following equation which is slightly different from Eq. (39).

$$\Omega_b{}^2 = 16\,sin^2\left(\frac{ak_w}{2}\right)tan^2\left(\frac{ak_w}{2}\right) \tag{44}$$

For an infinite number of grains, the granular chain asymptotically behaves as a gradient elasticity Rayleigh model (where the bending interactions are predominant). Eq. (40) with terms of translation and rotation inertia leads to

$$[\boldsymbol{EI\partial_x^4 - \rho I\partial_t^2\partial_x^2 + \rho A\partial_t^2}]\boldsymbol{w} = \boldsymbol{0} \tag{45}$$

Lu et al. [37] investigated the wave propagation properties in a nonlocal Euler-Bernoulli beam (Eq. (46)), based on a differential nonlocal model introduced by Eringen [5] for one-dimensional media. Eq. (45) could be compared well by Lu et al. [37] which obtained in their study as follows

$$\left[\boldsymbol{EI\partial_x^4 - \rho A\partial_t}^2((\boldsymbol{e_0 d_0})^2\boldsymbol{\partial_x^2} - \boldsymbol{1})\right]\boldsymbol{w} = \boldsymbol{0} \tag{46}$$

e_0 is the nondimensional calibration parameter of the Eringen nonlocal approach. This parameter adjusts in order to achieve a good dispersive curve at the end of the Brillouin zone and d_0 is an internal characteristic length. Eq. (46) is equivalent to considering an Eringen's based nonlocal model by

$$\boldsymbol{M - l_c^2 M'' = EIw''} \quad ; \quad \boldsymbol{M'' = -\rho A\ddot{w}} \tag{47}$$

Here l_c is the characteristic length of the nonlocal model. Regarding the fourth-order differential equation of the nonlocal beam (Eq. (46)) and considering the solution of the deflection in a harmonic form, by substituting Eq. (11) in Eq. (47), one could obtain:

$$\boldsymbol{EI{k_w}^4 - \rho A\omega^2(1 + (ae_0 k_w)^2) = 0} \tag{48}$$

in which e_0 could be defined by $e_0 = l_c/a$. The approximate angular frequencies calculated from Eringen's nonlocal beam approach could be obtained by:

$$\boldsymbol{{\Omega_b}^2 = \frac{(ak_w)^4}{1 + (ak_w)^2 {e_0}^2}} \tag{49}$$

where $\boldsymbol{\Omega_b}$ is the dimensionless parameter of frequency regarding to the bending wave velocity definition. Comparing Eq. (49) with the one issued of Eringen's model (Eringen [5]) applied to beam mechanics, (Eq. (39)) leads to the two fundamental values that differ for the low and high natural frequencies. These two values are obtained as follows

$$\textbf{for } ak_w \to 0: \quad (ak_w)^4\left(1-\frac{(ak_w)^2}{24}\right)^4=\frac{(ak_w)^4}{1+(ak_w)^2{e_0}^2}\Rightarrow e_0=\sqrt{\frac{1}{6}}\approx 0.408 \tag{50}$$

$$\textbf{for } ak_w=\pi: \quad 16=\frac{\pi^4}{1+(\pi)^2(e_0)^2}\Rightarrow e_0=\sqrt{\frac{\pi^2}{16}-\frac{1}{\pi^2}}\approx 0.718 \tag{51}$$

The specific values of e_0 =*0.408* and e_0 =*0.718* obtained in Eq. (50) and (51) could be verified well also by Challamel et al. [38].

Assuming only shear effects ($E \to 0$) and omitting Winkler foundation ($k = 0$), Eq. (6) leads to

$$[(A\delta_0 - I\delta_2){\partial_t}^2+\frac{\rho I{\partial_t}^4}{K_sG}]w_i=0 \tag{52}$$

This equation leads to the following relation by using Eq. (4)

$$\beta e^{j(\omega t-k_w x_i)}[I\left(e^{ak_wj}-2+e^{-ak_wj}\right)-\frac{Aa^2}{4}\left(e^{ak_wj}+2+e^{-ak_wj}\right)+\frac{\rho Ia^2}{K_sG}\omega^2]=0 \tag{53}$$

Which can be simplified as

$$4\,sin^2\left(\frac{ak_w}{2}\right)+\frac{Aa^2}{I}cos^2\left(\frac{ak_w}{2}\right)-\frac{\rho a^2}{K_sG}\omega^2=0 \tag{54}$$

Using Eq. (19) for the non-dimensional frequency with c_{shear}, one could be found as follows

$${\Omega_s}^2=4\,sin^2\left(\frac{ak_w}{2}\right)+\frac{1}{r^{*2}}cos^2\left(\frac{ak_w}{2}\right) \tag{55}$$

3.2. Exact Continuous Approach

From the continuum model, the wave propagation equation regarding the local Bresse-Timoshenko could be obtained as:

$$[EI{\partial_x}^4+\left(-\rho I{\partial_t}^2-\frac{kEI}{K_sGA}-\frac{EI\rho{\partial_t}^2}{K_sG}\right){\partial_x}^2+\left(k+\rho A{\partial_t}^2\right)+\frac{k\rho I{\partial_t}^2}{K_sGA}+\frac{\rho^2 I{\partial_t}^4}{K_sG}]w=0 \tag{56}$$

Substituting the fundamental solution of $w = We^{j(\omega t - k_w x)}$ (the wave propagation equation in the harmonic form for the continuum beam model) in Eq. (56) leads to:

$$\left(\frac{\boldsymbol{\rho^2}}{\boldsymbol{EK_sG}}\right)\boldsymbol{\omega^4} - (\left(\frac{\boldsymbol{\rho}}{\boldsymbol{E}} + \frac{\boldsymbol{\rho}}{\boldsymbol{K_sG}}\right)\left(\boldsymbol{k_w}^2\right) + \frac{\boldsymbol{\rho A}}{\boldsymbol{EI}} + \frac{\boldsymbol{k\rho}}{\boldsymbol{EK_sGA}})\boldsymbol{\omega^2} + \left(\boldsymbol{k_w}^4 + \frac{\boldsymbol{k}}{\boldsymbol{K_sGA}}\left(\boldsymbol{k_w}^2\right) + \frac{\boldsymbol{k}}{\boldsymbol{EI}}\right) = \boldsymbol{0} \tag{57}$$

On the other hand, for an infinite number of grains assuming $a \to 0$, the discrete dispersive relation of Eq. (13) leads to the biquadratic equation of Eq. (57). This dispersion equation for the continuum beam can be compared well also by the one obtained by Manevich [32] on Winkler elastic foundations (Eq. (18)).

3.3. Continuous Approach via Polynomial Expansion

In this section, the continualization of the difference equation of Eq. (6) is investigated using polynomial expansions. The finite difference terms are replaced by the corresponding Taylor series and lead to a Cosserat continuum theory.

Using this nonlocal solution allows to obtain the continuous approximate model of the discrete equations holds for a sufficiently smooth deflection function (Salvadori [39])(see for instance the application of this method for nonlinear lattices by Kruskal and Zabusky [40]):

$$\boldsymbol{w_i = w(x = ia)},$$

$$\boldsymbol{w_{i+1}} = \sum_{\boldsymbol{k=0}}^{\boldsymbol{\infty}} \frac{\boldsymbol{a^k \partial_x^k}}{\boldsymbol{k!}} \boldsymbol{w(x)} = \left[\boldsymbol{1} + \frac{\boldsymbol{a\partial_x^1}}{\boldsymbol{1!}} + \frac{\boldsymbol{a^2\partial_x^2}}{\boldsymbol{2!}} + \frac{\boldsymbol{a^3\partial_x^3}}{\boldsymbol{3!}} + \cdots\right]\boldsymbol{w(x)} = \boldsymbol{e^{a\partial_x} w(x)};\ \mathbf{x = ia} \tag{58}$$

The pseudodifferential operators ${\delta_2}^2, \delta_2$ and δ_0 could be expanded as:

$$\boldsymbol{{\delta_2}^2 w} = \left(\frac{\boldsymbol{e^{2a\partial_x} - 4e^{a\partial_x} + 6 - 4e^{-a\partial_x} + e^{-2a\partial_x}}}{\boldsymbol{a^4}}\right)\boldsymbol{w} = \left(\boldsymbol{1} + \frac{\boldsymbol{a^2\partial_x^2}}{\boldsymbol{6}} + \frac{\boldsymbol{a^4\partial_x^4}}{\boldsymbol{80}} + \frac{\boldsymbol{17a^6\partial_x^6}}{\boldsymbol{30240}} + \boldsymbol{O(a^8\partial_x^8)}\right)\boldsymbol{\partial_x^4 w},$$

$$\boldsymbol{\delta_2 w} = \left(\frac{\boldsymbol{e^{a\partial_x} - 2 + e^{-a\partial_x}}}{\boldsymbol{a^2}}\right)\boldsymbol{w} = \left(\boldsymbol{1} + \frac{\boldsymbol{a^2\partial_x^2}}{\boldsymbol{12}} + \frac{\boldsymbol{a^4\partial_x^4}}{\boldsymbol{360}} + \frac{\boldsymbol{a^6\partial_x^6}}{\boldsymbol{20160}} + \boldsymbol{O(a^8\partial_x^8)}\right)\boldsymbol{\partial_x^2 w},$$

$$\boldsymbol{\delta_0 w = \left(\frac{e^{a\partial_x}+2+e^{-a\partial_x}}{4}\right) w = \left(1+\frac{a^2\partial_x^2}{4}+\frac{a^4\partial_x^4}{48}+\frac{a^6\partial_x^6}{1440}+O(a^8\partial_x^8)\right) w} \tag{59}$$

A continualization procedure up to the order $\boldsymbol{a^6}$ from the difference equation of Eq. (6) through the substitution of the expansion series of Eq. (59) leads to the following higher-order gradient system:

$$\begin{aligned}\Bigg[EI\left(1+\frac{a^2}{6}\partial_x^2+\frac{a^4}{80}\partial_x^4+\frac{17a^6\partial_x^6}{30240}\right)\partial_x^4 \\ -\left(\rho I\partial_t{}^2+\frac{kEI}{K_sGA}+\frac{EI\rho}{K_sG}\partial_t{}^2\right)\left(1+\frac{a^2}{12}\partial_x^2+\frac{a^4}{360}\partial_x^4+\frac{a^6\partial_x^6}{20160}\right)\partial_x^2 \\ +\left(k+\rho A\partial_t{}^2\right)\left(1+\frac{a^2}{4}\partial_x^2+\frac{a^4\partial_x^4}{48}+\frac{a^6\partial_x^6}{1440}\right)+\left(\frac{k\rho I}{K_sGA}\partial_t{}^2+\frac{\rho^2 I}{K_sG}\partial_t{}^4\right)\Bigg] w=0\end{aligned} \tag{60}$$

which leads to the following nonlocal dispersion equation:

$$\begin{aligned}\left[\frac{17EIa^6}{30240}\right]w^{(10)}+\left[\frac{EIa^4}{80}-\left(\rho I\partial_t{}^2+\frac{kEI}{K_sGA}+\frac{EI\rho}{K_sG}\partial_t{}^2\right)\frac{a^6}{20160}\right]w^{(8)}+\left[\frac{EIa^2}{6}-\left(\rho I\partial_t{}^2+\frac{kEI}{K_sGA}+\right.\right. \\ \left.\left.\frac{EI\rho}{K_sG}\partial_t{}^2\right)\frac{a^4}{360}+\left(k+\rho A\partial_t{}^2\right)\frac{a^6}{1440}\right]w^{(6)}+\left[EI-\left(\rho I\partial_t{}^2+\frac{kEI}{K_sGA}+\frac{EI\rho}{K_sG}\partial_t{}^2\right)\frac{a^2}{12}+\left(k+\right.\right. \\ \left.\left.\rho A\partial_t{}^2\right)\frac{a^4}{48}\right]w^{(4)}+\left[-\left(\rho I\partial_t{}^2+\frac{kEI}{K_sGA}+\frac{EI\rho}{K_sG}\partial_t{}^2\right)+\left(k+\rho A\partial_t{}^2\right)\frac{a^2}{4}\right]w^{(2)}+\left[\left(k+\rho A\partial_t{}^2\right)+\right. \\ \left.\frac{k\rho I}{K_sGA}\partial_t{}^2+\frac{\rho^2 I}{K_sG}\partial_t{}^4\right]w=0\end{aligned} \tag{61}$$

To satisfy this eighth-order differential equation, a wave equation in a harmonic type is chosen again as Eq. (11). One would be obtained as:

$$\left[\frac{\rho^2}{EK_sG}\right]\omega^4 - \left[-\left(\frac{\rho}{E}+\frac{\rho}{K_sG}\right)\left(\frac{a^6}{20160}\right)k_w{}^8 + \left(\left(\frac{\rho}{E}+\frac{\rho}{K_sG}\right)-\left(\frac{\rho A}{EI}\right)\left(\frac{a^2}{4}\right)\right)\left(\left(\frac{a^4}{360}\right)k_w{}^6 - \left(\frac{a^2}{12}\right)k_w{}^4 + k_w{}^2\right) + \left(\frac{\rho A}{EI}+\frac{k\rho}{EK_sGA}\right)\right]\omega^2 + \left[-\left(\frac{17a^6}{30240}\right)k_w{}^{10} + \left(\frac{a^4}{80}-\frac{ka^6}{20160K_sGA}\right)k_w{}^8 + \left(-\frac{ka^6}{1440EI}+\frac{ka^4}{360K_sGA}-\frac{a^2}{6}\right)k_w{}^6 + \left(1-\frac{ka^2}{12K_sGA}+\frac{ka^4}{48EI}\right)k_w{}^4 + \left(\frac{k}{K_sGA}-\frac{ka^2}{4EI}\right)k_w{}^2 + \frac{k}{EI}\right] = 0 \quad (62)$$

which could be rewritten through the dimensionless parameters of Eq. (19) as follows:

$$\Omega_b{}^4 - \left[\left(\frac{1}{\mu_s r^{*2}}+\frac{1}{r^{*2}}\right)\left(-\frac{(ak_w)^8}{20160}+\frac{(ak_w)^6}{360}-\frac{(ak_w)^4}{12}+(ak_w)^2\right) + \left(\frac{1}{\mu_s r^{*4}}\right)\left(-\frac{(ak_w)^6}{1440}+\frac{(ak_w)^4}{48}-\frac{(ak_w)^2}{4}+1\right)+k^*\right]\Omega_b{}^2 + \left[\left(\frac{1}{\mu_s r^{*4}}\right)\left(-\frac{17(ak_w)^{10}}{30240}+\frac{(ak_w)^8}{80}-\frac{(ak_w)^6}{6}+(ak_w)^4\right) + \left(\frac{k^*}{r^{*2}}\right)\left(-\frac{(ak_w)^8}{20160}+\frac{(ak_w)^6}{360}-\frac{(ak_w)^4}{12}+(ak_w)^2\right) + \left(\frac{k^*}{\mu_s r^{*4}}\right)\left(-\frac{(ak_w)^6}{1440}+\frac{(ak_w)^4}{48}-\frac{(ak_w)^2}{4}+1\right)\right] = 0 \quad (63)$$

While for the fourth order continualization, neglecting the terms of a^6, Eq. (62) could be simplified to the following quartic equation:

$$\left[\frac{\rho^2}{EK_sG}\right]\omega^4 - \left[\left(\frac{\rho}{E}+\frac{\rho}{K_sG}\right)\left(\left(\frac{a^4}{360}\right){k_w}^6 - \left(\frac{a^2}{12}\right){k_w}^4 + {k_w}^2\right) + \left(\frac{\rho A}{EI}\right)\left(\left(\frac{a^4}{48}\right){k_w}^4 - \left(\frac{a^2}{4}\right){k_w}^2 + 1\right) + \left(\frac{k\rho}{EK_sGA}\right)\right]\omega^2 + \left[\left(\frac{a^4}{80}\right){k_w}^8 + \left(\frac{ka^4}{360K_sGA} - \frac{a^2}{6}\right){k_w}^6 + \left(1 - \frac{ka^2}{12K_sGA} + \frac{ka^4}{48EI}\right){k_w}^4 + \left(\frac{k}{K_sGA} - \frac{ka^2}{4EI}\right){k_w}^2 + \frac{k}{EI}\right] = 0 \quad (64)$$

Using the dimensionless parameters of Eq. (19) leads to:

$$\Omega_b{}^4 - \left[\left(\frac{1}{\mu_s r^{*2}}+\frac{1}{r^{*2}}\right)\left(\frac{(ak_w)^6}{360} - \frac{(ak_w)^4}{12} + (ak_w)^2\right) + \left(\frac{1}{\mu_s r^{*4}}\right)\left(\frac{(ak_w)^4}{48} - \frac{(ak_w)^2}{4} + 1\right) + k^*\right]\Omega_b{}^2 + \left[\left(\frac{1}{\mu_s r^{*4}}\right)\left(\frac{(ak_w)^8}{80} - \frac{(ak_w)^6}{6} + (ak_w)^4\right) + \left(\frac{k^*}{r^{*2}}\right)\left(\frac{(ak_w)^6}{360} - \frac{(ak_w)^4}{12} + (ak_w)^2\right) + \left(\frac{k^*}{\mu_s r^{*4}}\right)\left(\frac{(ak_w)^4}{48} - \frac{(ak_w)^2}{4} + 1\right)\right] = 0 \quad (65)$$

Using the second order a^2 of the continualization of the Taylor expansion series of Eq. (59), the difference equation of Eq. (6) leads to the following higher-order gradient system:

$$\left[EI\left(1+\frac{a^2}{6}\partial_x^2\right)\partial_x^4 - \left(\rho I\partial_t{}^2 + \frac{kEI}{K_sGA} + \frac{EI\rho}{K_sG}\partial_t{}^2\right)\left(1+\frac{a^2}{12}\partial_x^2\right)\partial_x^2 + \left(k+\rho A\partial_t{}^2\right)\left(1+\frac{a^2}{4}\partial_x^2\right) + \left(\frac{k\rho I}{K_sGA}\partial_t{}^2 + \frac{\rho^2 I}{K_sG}\partial_t{}^4\right)\right]w = 0 \quad (66)$$

For the static range, this equation leads to the one obtained by Challamel et al. [13]. Using the dimensionless parameters introduced in Eq. (19), the comparable deflection equation of the continuous approximate for the static condition would be obtained as follows

$$\left[\left(1+\frac{a^2}{6}\partial_x^2\right)\partial_x^4 - k^*\mu_s r^{*2}\left(1+\frac{a^2}{12}\partial_x^2\right)\partial_x^2 + k^*\left(1+\frac{a^2}{4}\partial_x^2\right)\right]\bar{w} = 0 \quad (67)$$

where $w = \frac{\bar{w}}{a}$. Let's consider the case of a granular chain with predominant bending interactions ($S \to \infty$). Thus, Eq. (66) leads to

$$\left[EI\left(1+\frac{a^2}{6}\partial_x^2\right)\partial_x^4 - \left(\rho I\partial_t{}^2\right)\left(1+\frac{a^2}{12}\partial_x^2\right)\partial_x^2 + \left(k+\rho A\partial_t{}^2\right)\left(1+\frac{a^2}{4}\partial_x^2\right)\right]w = 0 \tag{68}$$

This gradient elasticity Rayleigh model (pure bending) under a gradient Winkler elastic foundation is associated with a non-positive definite energy function. After integration by part, one obtains the following energy functional:

$$\begin{aligned}\Pi = \int \frac{1}{2}EI\left(w''^2 - \frac{a^2}{6}w'''^2\right)dx + \int \frac{1}{2}\rho I\partial_t{}^2\left(w'^2 - \frac{a^2}{12}w''^2\right)dx \\ + \int \frac{1}{2}\left(k+\rho A\partial_t{}^2\right)\left(w^2 - \frac{a^2}{4}w'^2\right)dx.\end{aligned} \tag{69}$$

The wave propagation equation could be obtained as the following sixth-order differential equation from Eq. (66):

$$\begin{aligned}\left[\frac{EIa^2}{6}\right]w^{(6)} + \left[EI - \left(\rho I\partial_t{}^2 + \frac{kEI}{K_sGA} + \frac{EI\rho}{K_sG}\partial_t{}^2\right)\frac{a^2}{12}\right]w^{(4)} + \left[-\left(\rho I\partial_t{}^2 + \frac{kEI}{K_sGA} + \frac{EI\rho}{K_sG}\partial_t{}^2\right) + \right. \\ \left.\left(k+\rho A\partial_t{}^2\right)\frac{a^2}{4}\right]w^{(2)} + \left[\left(k+\rho A\partial_t{}^2\right) + \frac{k\rho I}{K_sGA}\partial_t{}^2 + \frac{\rho^2 I}{K_sG}\partial_t{}^4\right]w = 0\end{aligned} \tag{70}$$

Again, using a wave equation in a harmonic type like Eq. (11) leads to:

$$\begin{aligned}\left[\frac{\rho^2}{EK_sG}\right]\omega^4 + \left[\left(\frac{\rho}{E}+\frac{\rho}{K_sG}\right)\left(\frac{a^2}{12}\right)k_w{}^4 + \left(\frac{\rho Aa^2}{4EI} - \frac{\rho}{E} - \frac{\rho}{K_sG}\right)k_w{}^2 - \left(\frac{\rho A}{EI} + \frac{k\rho}{EK_sGA}\right)\right]\omega^2 \\ + \left[-\left(\frac{a^2}{6}\right)k_w{}^6 + \left(1 - \frac{ka^2}{12K_sGA}\right)k_w{}^4 + \left(\frac{k}{K_sGA} - \frac{ka^2}{4EI}\right)k_w{}^2 + \frac{k}{EI}\right] = 0\end{aligned} \tag{71}$$

and in the nondimensional form as:

$$\Omega_b{}^4 + \left[\left(\frac{1}{\mu_s r^{*2}} + \frac{1}{r^{*2}}\right)\frac{(ak_w)^4}{12} + \left(\frac{1}{4\mu_s r^{*4}} - \frac{1}{\mu_s r^{*2}} - \frac{1}{r^{*2}}\right)(ak_w)^2 - \left(\frac{1}{\mu_s r^{*4}} + k^*\right)\right]\Omega_b{}^2$$
$$+ \left[-\left(\frac{1}{\mu_s r^{*4}}\right)\frac{(ak_w)^6}{6} + \left(\frac{1}{\mu_s r^{*4}} - \frac{k^*}{12r^{*2}}\right)(ak_w)^4 + \left(\frac{k^*}{r^{*2}} - \frac{k^*}{4\mu_s r^{*4}}\right)(ak_w)^2\right.$$
$$\left. + \frac{k^*}{\mu_s r^{*4}}\right] = 0 \qquad (72)$$

The dispersive analysis of the granular chain with regards to the dimensionless parameter of bending frequency is done for the two branches. The results are plotted in Fig. 2 asymptotically for a numeral example characterized in Eq. (73) through the equations obtained for discrete exact, local continuum and nonlocal Taylor approaches (Eq. (13), (62), (64), (57) and (71)). For instance, in order to investigate a sensitive numerical analysis of the abovementioned model, we consider the following parameters (steel is assumed for the material parameter). Let's assume the mechanical parameters of steel with an elastic foundation as follows

$$E = 200\ GPa,\ G = 70\ GPa,\ K_s = 0.667,\ \rho = 8000\ \frac{kg}{m^3},\ k = 50\ MPa. \qquad (73)$$

(a) (b)

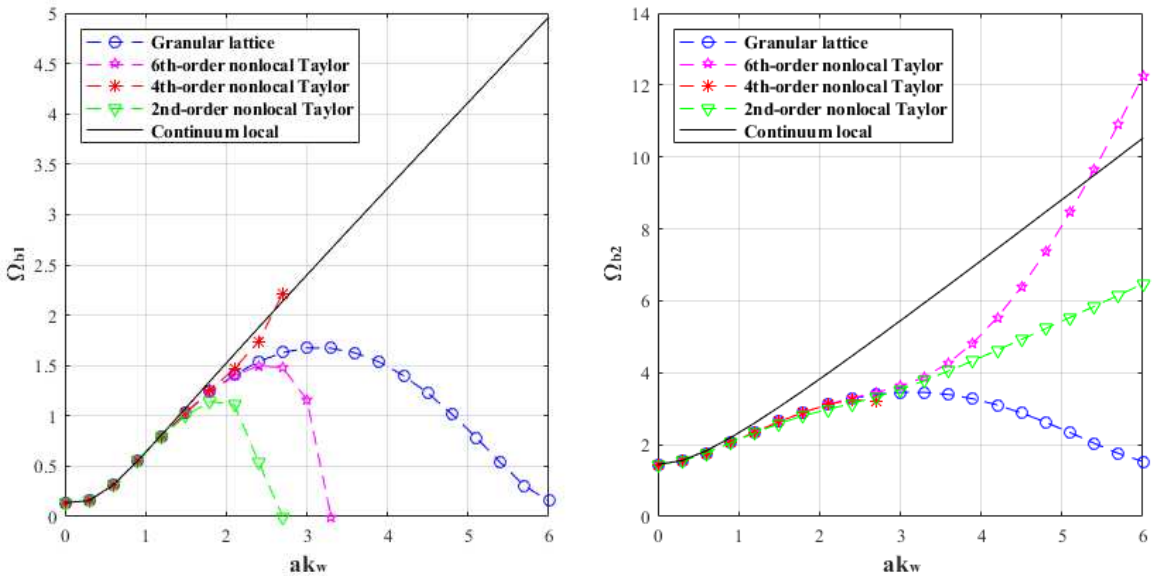

Fig. 2. Dispersive curves for one-dimensional compression wave of (a) first branch and (b)second branch according to bending nondimensional parameter for $\mu_s = 4.28$, $r^* = 0.289$ and $k^* = 0.02$.

Due to the quartic equation of Eq. (62), depending on the discriminant value of this equation for the sixth, the fourth and the second order expansion of Taylor series, the dynamic results could take complex values.

For analyzing the behavior of the nonlocal approach using the Taylor development precisely, here an asymptotic study of the frequency has been done. Regarding to Eq. (63),one could be obtained for the dimensionless parameter of bending frequency as follows:

$$\boldsymbol{\Omega_b = \sqrt{\varepsilon \pm \sqrt{\varepsilon^2 - \gamma}}} \tag{74}$$

where ε and γ would be considered as

$$\boldsymbol{\varepsilon = \frac{1}{2}\left[\left(\frac{1}{\mu_s r^{*2}} + \frac{1}{r^{*2}}\right)\left(-\frac{(ak_w)^8}{20160} + \frac{(ak_w)^6}{360} - \frac{(ak_w)^4}{12} + (ak_w)^2\right) + \left(\frac{1}{\mu_s r^{*4}}\right)\left(-\frac{(ak_w)^6}{1440} + \frac{(ak_w)^4}{48} - \frac{(ak_w)^2}{4} + 1\right) + k^*\right],}$$

$$\boldsymbol{\gamma = \left(\frac{1}{\mu_s r^{*4}}\right)\left(-\frac{17(ak_w)^{10}}{30240} + \frac{(ak_w)^8}{80} - \frac{(ak_w)^6}{6} + (ak_w)^4\right) + \left(\frac{k^*}{r^{*2}}\right)\left(-\frac{(ak_w)^8}{20160} + \frac{(ak_w)^6}{360} - \frac{(ak_w)^4}{12} + (ak_w)^2\right) + \left(\frac{k^*}{\mu_s r^{*4}}\right)\left(-\frac{(ak_w)^6}{1440} + \frac{(ak_w)^4}{48} - \frac{(ak_w)^2}{4} + 1\right)} \tag{75}$$

Due to the discriminant of Eq. (74) and the typical values for the mechanical and geometrical parameters of the system (Eq. (73)) the results contain the imaginary part. Fig. 3 clarifies this evidence as follows

(a)

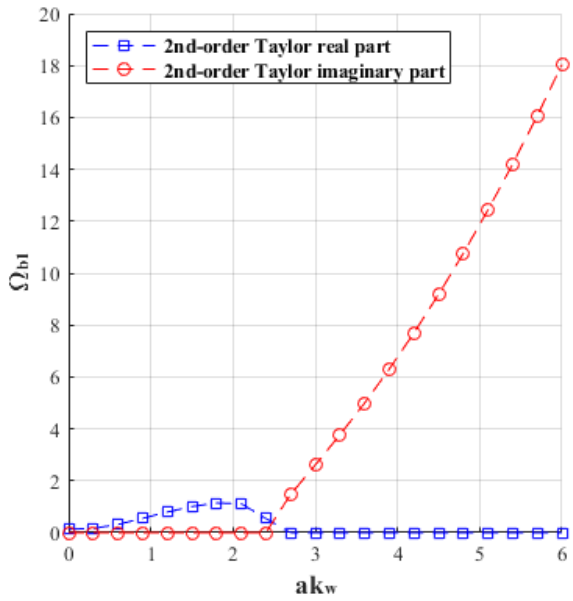

(b)

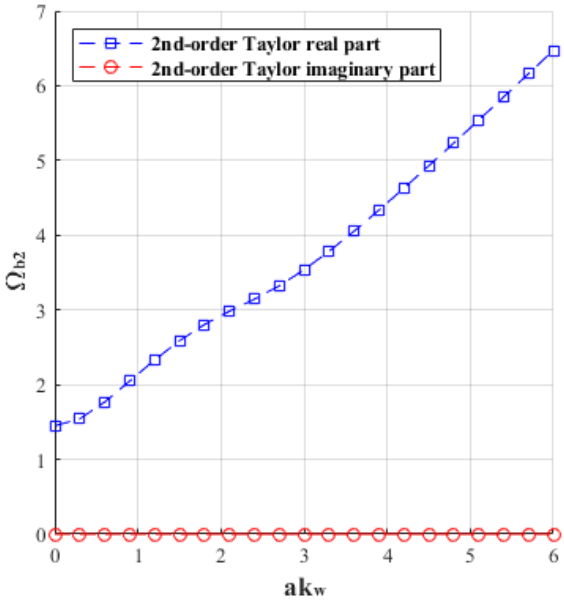

(c)

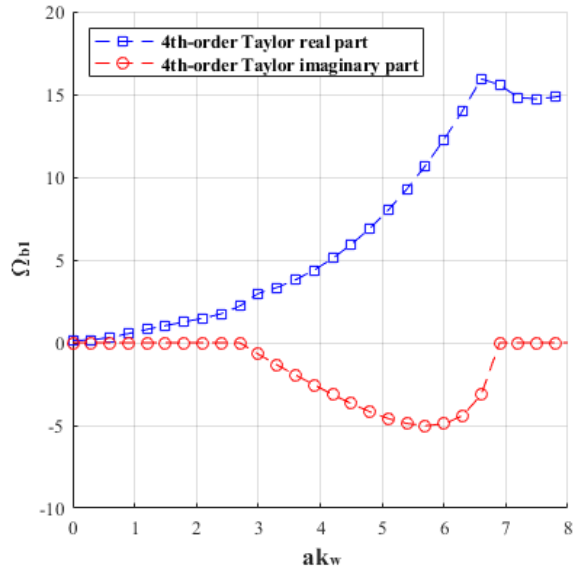

(d)

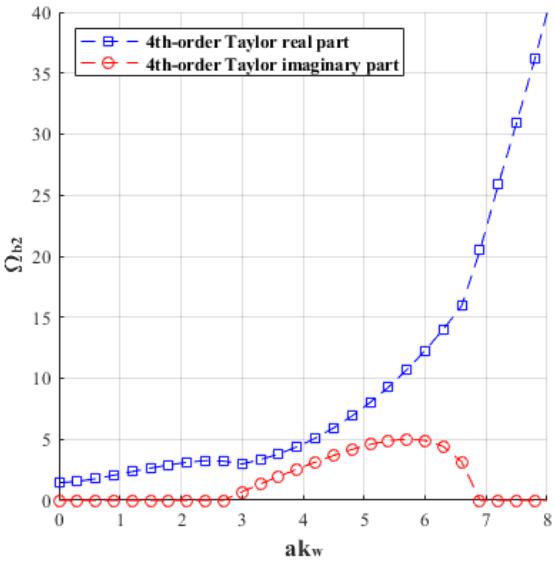

(e) (f)

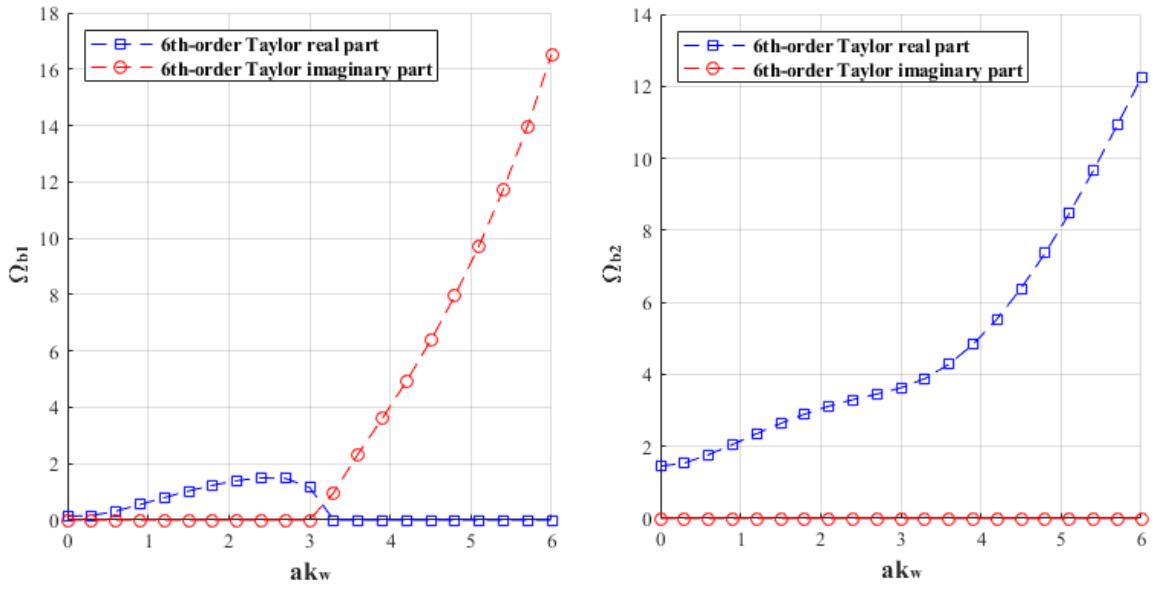

Fig. 3. The complex results of nonlocal Taylor development (a) 2nd-order first branch, (b) 2nd-order second branch, (c) 4th-order first branch, (d) 4th-order second branch, (e) 6th-order first branch and (f) 6th -order second branch according to bending nondimensional parameter for $\mu_s = 4.28$, $r^* = 0.289$ and $k^* = 0.02$.

3.4. Continuous Approach via Rational Expansion

Another nonlocal approximation is based on a rational expansion (Padé approximants) instead of the polynomial approximation, that may lead to a better-homogenized solution in comparison to the Taylor series (Duan et al. [35]). With the application of Padé approximant of order in $\boldsymbol{a^4}$ subsequently for the pseudo-differential operators of Eq. (59), ones would be obtained as:

$$\boldsymbol{\delta_2{}^2 w \approx \left(1 - \frac{a^2\partial_x^2}{6} + \frac{11a^4\partial_x^4}{720}\right)^{-1} \partial_x^4 w,}$$

$$\boldsymbol{\delta_2 w(x) \approx \left(1 - \frac{a^2\partial_x^2}{12} + \frac{a^4\partial_x^4}{240}\right)\left(1 - \frac{a^2\partial_x^2}{6} + \frac{11a^4\partial_x^4}{720}\right)^{-1} \partial_x^2 w,}$$

$$\boldsymbol{\delta_0 w \approx \left(1+\frac{a^2\partial_x^2}{12}-\frac{a^4\partial_x^4}{180}\right)\left(1-\frac{a^2\partial_x^2}{6}+\frac{11a^4\partial_x^4}{720}\right)^{-1} w} \tag{76}$$

Thus, the deflection equation of Eq. (6) for a discrete system could be written for a continuous system using Eq. (76) as:

$$\left[\frac{1}{1-\frac{a^2\partial_x^2}{6}+\frac{11a^4\partial_x^4}{720}}\partial_x^4-\left(\left(\frac{\rho}{E}+\frac{\rho}{K_sG}\right)\partial_t{}^2+\frac{k}{K_sGA}\right)\frac{1-\frac{a^2\partial_x^2}{12}+\frac{a^4\partial_x^4}{240}}{1-\frac{a^2\partial_x^2}{6}+\frac{11a^4\partial_x^4}{720}}\partial_x^2+\left(\frac{k}{EI}+\frac{\rho A}{EI}\partial_t{}^2\right)\frac{1+\frac{a^2\partial_x^2}{12}-\frac{a^4\partial_x^4}{180}}{1-\frac{a^2\partial_x^2}{6}+\frac{11a^4\partial_x^4}{720}}+\left(\frac{k\rho}{EK_sGA}\partial_t{}^2+\frac{\rho^2}{EK_sG}\partial_t{}^4\right)\right]w=0 \tag{77}$$

Multiplying Eq. (77) by $(1-\frac{a^2\partial_x^2}{6}+\frac{11a^4\partial_x^4}{720})$ leads to the following compact form equation:

$$\left[\partial_x^4-\left(\left(\frac{\rho}{E}+\frac{\rho}{K_sG}\right)\partial_t{}^2+\frac{k}{K_sGA}\right)\left(1-\frac{a^2\partial_x^2}{12}+\frac{a^4\partial_x^4}{240}\right)\partial_x^2+\left(\frac{k}{EI}+\frac{\rho A}{EI}\partial_t{}^2\right)\left(1+\frac{a^2\partial_x^2}{12}-\frac{a^4\partial_x^4}{180}\right)+\left(\frac{k\rho}{EK_sGA}\partial_t{}^2+\frac{\rho^2}{EK_sG}\partial_t{}^4\right)\left(1-\frac{a^2\partial_x^2}{6}+\frac{11a^4\partial_x^4}{720}\right)\right]w=0 \tag{78}$$

The wave propagation equation can be obtained by:

$$\begin{aligned}&\left[-\left(\left(\frac{\rho}{E}+\frac{\rho}{K_sG}\right)\partial_t{}^2+\frac{k}{K_sGA}\right)\left(\frac{a^4}{240}\right)\right]\partial_x^6 w\\&+\left[1+\left(\left(\frac{\rho}{E}+\frac{\rho}{K_sG}\right)\partial_t{}^2+\frac{k}{K_sGA}\right)\left(\frac{a^2}{12}\right)-\left(\frac{k}{EI}+\frac{\rho A}{EI}\partial_t{}^2\right)\left(\frac{a^4}{180}\right)\right.\\&\left.+\left(\frac{k\rho}{EK_sGA}\partial_t{}^2+\frac{\rho^2}{EK_sG}\partial_t{}^4\right)\left(\frac{11a^4}{720}\right)\right]\partial_x^4 w\\&-\left[\left(\left(\frac{\rho}{E}+\frac{\rho}{K_sG}\right)\partial_t{}^2+\frac{k}{K_sGA}\right)-\left(\frac{k}{EI}+\frac{\rho A}{EI}\partial_t{}^2\right)\left(\frac{a^2}{12}\right)\right.\\&\left.+\left(\frac{k\rho}{EK_sGA}\partial_t{}^2+\frac{\rho^2}{EK_sG}\partial_t{}^4\right)\left(\frac{a^2}{6}\right)\right]\partial_x^2 w\\&+\left[\left(\frac{k}{EI}+\frac{\rho A}{EI}\partial_t{}^2\right)+\left(\frac{k\rho}{EK_sGA}\partial_t{}^2+\frac{\rho^2}{EK_sG}\partial_t{}^4\right)\right]w=0\end{aligned} \tag{79}$$

Applying the fundamental solution of Eq. (11), the characteristic equation of the nonlocal continued model (nonlocal model Padé 1) is obtained as follows

$$\begin{aligned}
&\left[\frac{\rho^2}{EK_sG}\left(\frac{11a^4}{720}{k_w}^4+\frac{a^2}{6}{k_w}^2+1\right)\right]\omega^4\\
&\quad-\left[\left(\left(\frac{\rho}{E}+\frac{\rho}{K_sG}\right)\frac{a^4}{240}\right){k_w}^6+\left(\left(\frac{\rho}{E}+\frac{\rho}{K_sG}\right)\frac{a^2}{12}+\left(\frac{k\rho}{EK_sGA}-\frac{4\rho A}{11EI}\right)\frac{11a^4}{720}\right){k_w}^4\right.\\
&\quad\left.+\left(\frac{\rho}{E}+\frac{\rho}{K_sG}+\left(\frac{k\rho}{EK_sGA}-\frac{\rho A}{2EI}\right)\frac{a^2}{6}\right){k_w}^2+\left(\frac{\rho A}{EI}+\frac{k\rho}{EK_sGA}\right)\right]\omega^2\\
&\quad+\left[\left(\left(\frac{k}{K_sGA}\right)\frac{a^4}{240}\right){k_w}^6+\left(1+\left(\frac{k}{K_sGA}\right)\frac{a^2}{12}-\left(\frac{k}{EI}\right)\frac{a^4}{180}\right){k_w}^4\right.\\
&\quad\left.+\left(\frac{k}{K_sGA}-\left(\frac{k}{EI}\right)\frac{a^2}{12}\right){k_w}^2+\frac{k}{EI}\right]=0
\end{aligned}\tag{80}$$

The dimensionless form of this equation would be obtained through the dimensionless parameters of Eq. (19) as follows:

$$\begin{aligned}
&\left[\left(\frac{11(ak_w)^4}{720}+\frac{(ak_w)^2}{6}+1\right)\right]{\Omega_b}^4\\
&\quad-\left[\left(\frac{1}{\mu_s{r^*}^2}+\frac{1}{{r^*}^2}\right)\frac{(ak_w)^6}{240}+\left(\left(\frac{1}{\mu_s{r^*}^2}+\frac{1}{{r^*}^2}\right)\frac{1}{12}+\left(k^*-\frac{4}{11\mu_s{r^*}^4}\right)\frac{11}{720}\right)(ak_w)^4\right.\\
&\quad\left.+\left(\frac{1}{\mu_s{r^*}^2}+\frac{1}{{r^*}^2}+\left(k^*-\frac{1}{2\mu_s{r^*}^4}\right)\frac{1}{6}\right)(ak_w)^2+\left(\frac{1}{\mu_s{r^*}^4}+k^*\right)\right]{\Omega_b}^2\\
&\quad+\left[\left(\frac{k^*}{240{r^*}^2}\right)(ak_w)^6+\left(\frac{1}{\mu_s{r^*}^4}+\frac{k^*}{12{r^*}^2}-\frac{k^*}{180\mu_s{r^*}^4}\right)(ak_w)^4\right.\\
&\quad\left.+\left(\frac{k^*}{{r^*}^2}-\frac{k^*}{12\mu_s{r^*}^4}\right)(ak_w)^2+\frac{k^*}{\mu_s{r^*}^4}\right]=0
\end{aligned}\tag{81}$$

On the other hand, regarding the work of Bacigalupo and Gambarotta [41] or Bacigalupo and Gambarotta [42] by using the approach of enhanced continualization via the first-order regularization, the derivatives of the continuum fields could be expressed by

$$\partial_x \widetilde{w}_i = \frac{e^{a\partial_x} - e^{-a\partial_x}}{2a} w_i \tag{82}$$

And the down-scaling law for each node defined by

$$w_i = \frac{2a\partial_x}{e^{a\partial_x} - e^{-a\partial_x}} \widetilde{w}_i \tag{83}$$

Substituting Eq. (83) in Eq. (3) leads to

$$\begin{gathered}\left(2S\frac{(e^{a\partial_x} - (2 + ka/s) + e^{-a\partial_x})}{e^{a\partial_x} - e^{-a\partial_x}} a\partial_x\right)\widetilde{w}_i - a^2 S\partial_x\widetilde{\theta}_i - \left(\frac{2m}{e^{a\partial_x} - e^{-aD_x}} a\partial_x\right)\ddot{\widetilde{w}}_i = 0, \\ \left((C\frac{(e^{a\partial_x} - 2 + e^{-a\partial_x})}{e^{a\partial_x} - e^{-a\partial_x}} - \frac{a^2}{4}S\frac{(e^{a\partial_x} + 2 + e^{-a\partial_x})}{e^{a\partial_x} - e^{-a\partial_x}})2a\partial_x\right)\widetilde{\theta}_i + a^2 S\partial_x\widetilde{w}_i - \left(\frac{2I_m}{e^{a\partial_x} - e^{-a\partial_x}} a\partial_x\right)\ddot{\widetilde{\theta}}_i = 0\end{gathered} \tag{84}$$

Here, the differential equations of the equivalent homogenized continuum are obtained by applying the fourth-order terms of the Taylor series:

$$\begin{gathered}-kaw_i + \left(s + \frac{1}{6}ka\right)a^2\frac{\partial^2 w}{\partial x^2} - \left(\frac{s}{12} + \frac{7}{360}ka\right)a^4\frac{\partial^4 w}{\partial x^4} - aS\frac{\partial\theta}{\partial x} - m\left(\ddot{w} - \frac{a^2}{6}\frac{\partial^2\ddot{w}}{\partial x^2} + \frac{7a^4}{360}\frac{\partial^4\ddot{w}}{\partial x^4}\right) = 0, \\ -a^2 Sw_i + \left(C - \frac{a^2}{12}S\right)a^2\frac{\partial^2\theta_i}{\partial x^2} - \left(\frac{C}{12} + \frac{a^2}{144}S\right)a^4\frac{\partial^4\theta_i}{\partial x^4} + aS\frac{\partial w}{\partial x} - I_m\left(\ddot{\theta} - \frac{a^2}{6}\frac{\partial^2\ddot{\theta}}{\partial x^2} + \frac{7a^4}{360}\frac{\partial^4\ddot{\theta}}{\partial x^4}\right) = 0\end{gathered} \tag{85}$$

Regarding Eq. (83), the pseudo-difference operators of Eq. (4) actually could be expressed in the following form

$$\delta_2{}^2 w = \left(\frac{2a\partial_x}{e^{a\partial_x - e^{-a\partial_x}}}\right)\left(\frac{e^{2a\partial_x} - 4e^{a\partial_x} + 6 - 4e^{-a\partial_x} + e^{-2a\partial_x}}{a^4}\right)\widetilde{w} = \left(1 + \frac{a^4\partial_x^4}{240} + O(a^6\partial_x^6)\right)\partial_x^4\widetilde{w},$$

$$\delta_2 w = \left(\frac{2a\partial_x}{e^{a\partial_x} - e^{-a\partial_x}}\right)\left(\frac{e^{a\partial_x} - 2 + e^{-a\partial_x}}{a^2}\right)\widetilde{w} = \left(1 - \frac{a^2\partial_x^2}{12} + \frac{a^4\partial_x^4}{120} + O(a^6\partial_x^6)\right)\partial_x^2\widetilde{w},$$

$$\delta_1 w = \left(\frac{2a\partial_x}{e^{a\partial_x} - e^{-a\partial_x}}\right)\left(\frac{e^{a\partial_x} - e^{-a\partial_x}}{2a}\right)\widetilde{w} = \partial_x\widetilde{w},$$

$$\delta_0 w = \left(\frac{2a\partial_x}{e^{a\partial_x - e^{-a\partial_x}}}\right)\left(\frac{e^{a\partial_x} + 2 + e^{-a\partial_x}}{4}\right)\widetilde{w} = \left(1 + \frac{a^2\partial_x^2}{12} - \frac{a^4\partial_x^4}{720} + O(a^6\partial_x^6)\right)\widetilde{w} \tag{86}$$

Continualizing Eq. (6) through the application of the series of Eq. (86) and neglecting higher-order terms in a^4 leads to the following extended deflection equation

$$\left[EI\partial_x^4 - \left(\rho I{\partial_t}^2 + \frac{kEI}{K_sGA} + \frac{EI\rho}{K_sG}{\partial_t}^2\right)\left(1 - \frac{a^2\partial_x^2}{12}\right)\partial_x^2 + \left(k + \rho A{\partial_t}^2\right)\left(1 + \frac{a^2\partial_x^2}{12}\right) + \left(\frac{k\rho I{\partial_t}^2}{K_sGA} + \frac{\rho^2 I{\partial_t}^4}{K_sG}\right)\left(1 - \frac{a^2\partial_x^2}{6}\right)\right]\widetilde{w} = 0 \quad (87)$$

This equation (nonlocal model Padé 1) could be obtained also from Eq. (79) neglecting the higher-order terms in a^4. An alternative strategy to obtain Eq. (87) is through the multiplication of $\left(1 - \frac{a^2\partial_x^2}{6}\right)$ to Eq. (66). Eq. (87) would be simplified as:

$$\left[EI + \left(\rho I{\partial_t}^2 + \frac{kEI}{K_sGA} + \frac{EI\rho}{K_sG}{\partial_t}^2\right)\frac{a^2}{12}\right]\widetilde{w}^{(4)} - \left[\left(\rho I{\partial_t}^2 + \frac{kEI}{K_sGA} + \frac{EI\rho}{K_sG}{\partial_t}^2\right) - \left(k + \rho A{\partial_t}^2\right)\frac{a^2}{12} + \left(\frac{k\rho I{\partial_t}^2}{K_sGA} + \frac{\rho^2 I{\partial_t}^4}{K_sG}\right)\frac{a^2}{6}\right]\widetilde{w}^{(2)} + \left[k + \left(\rho A + \frac{k\rho I}{K_sGA} + \frac{\rho^2 I}{K_sG}{\partial_t}^2\right){\partial_t}^2\right]\widetilde{w} = 0 \quad (88)$$

Choosing again a wave equation in a harmonic type as Eq. (11), one would be obtained:

$$\left[\frac{\rho^2}{EK_sG}\left(1 + \frac{a^2}{6}{k_w}^2\right)\right]\omega^4 - \left[\left(\frac{\rho}{E} + \frac{\rho}{K_sG}\right)\left(\frac{a^2}{12}\right){k_w}^4 + \left(\frac{\rho}{E} + \frac{\rho}{K_sG} + \left(\frac{k\rho}{EK_sGA} - \frac{\rho A}{2EI}\right)\frac{a^2}{6}\right){k_w}^2 + \left(\frac{\rho A}{EI} + \frac{k\rho}{EK_sGA}\right)\right]\omega^2 + \left[\left(1 + \frac{ka^2}{12K_sGA}\right){k_w}^4 + \left(\frac{k}{K_sGA} - \frac{ka^2}{12EI}\right){k_w}^2 + \frac{k}{EI}\right] = 0 \quad (89)$$

Using Eq. (19), the following non-dimensional equation would be obtained through the bending wave velocity definition.

$$\left[\left(\frac{(ak_w)^2}{6} + 1\right)\right]{\Omega_b}^4 - \left[\left(\frac{1}{\mu_s {r^*}^2} + \frac{1}{{r^*}^2}\right)\frac{(ak_w)^4}{12} + \left(\frac{1}{\mu_s {r^*}^2} + \frac{1}{{r^*}^2} + \left(k^* - \frac{1}{2\mu_s {r^*}^4}\right)\frac{1}{6}\right)(ak_w)^2 + \left(\frac{1}{\mu_s {r^*}^4} + k^*\right)\right]{\Omega_b}^2 + \left[\left(\frac{1}{\mu_s {r^*}^4} + \frac{k^*}{12{r^*}^2}\right)(ak_w)^4 + \left(\frac{k^*}{{r^*}^2} - \frac{k^*}{12\mu_s {r^*}^4}\right)(ak_w)^2 + \frac{k^*}{\mu_s {r^*}^4}\right] = 0 \quad (90)$$

An alternative continuous approach could be obtained by multiplying the terms $\left(1-\frac{a^2\partial_x^2}{3}\right)$ to Eq. (66) and neglect higher-order terms in a^4. This leads to the following extended governed equation (nonlocal model Padé 2):

$$\left[EI\left(1-\frac{a^2}{6}\partial_x^2\right)\partial_x^4-\left(\rho I{\partial_t}^2+\frac{kEI}{K_sGA}+\frac{EI\rho}{K_sG}{\partial_t}^2\right)\left(1-\frac{a^2}{4}\partial_x^2\right)\partial_x^2+\left(k+\rho A{\partial_t}^2\right)\left(1-\frac{a^2}{12}\partial_x^2\right)\right.$$
$$\left.+\left(\frac{k\rho I}{K_sGA}{\partial_t}^2+\frac{\rho^2 I}{K_sG}{\partial_t}^4\right)\left(1-\frac{a^2}{3}\partial_x^2\right)\right]w=0 \tag{91}$$

Here, the gradient elasticity for a granular chain with predominant bending interactions are associated with positive definite energy function as follows:

$$\Pi=\int\frac{1}{2}EI\left(w''^2+\frac{a^2}{6}w'''^2\right)dx+\int\frac{1}{2}\rho I{\partial_t}^2\left(w'^2+\frac{a^2}{4}w''^2\right)dx$$
$$+\int\frac{1}{2}\left(k+\rho A{\partial_t}^2\right)\left(w^2+\frac{a^2}{12}w'^2\right)dx. \tag{92}$$

For the static analysis, the comparable deflection equation of the continuous approximate again leads to the one investigated by Challamel et al. [13] neglecting the compressional buckling force as follows

$$\left[\left(1-\frac{a^2}{6}D_x^2\right)D_x^4-k^*\mu_s r^{*2}\left(1-\frac{a^2}{4}D_x^2\right)D_x^2+k^*\left(1-\frac{a^2}{12}D_x^2\right)\right]\bar{w}=0 \tag{93}$$

Going back to the continuous approximate model expressed by the enriched differential equation (Eq. (91)), the wave propagation equation could be obtained as:

$$\left[\frac{EIa^2}{6}\right]w^{(6)} - \left[EI + \left(\rho I\partial_t{}^2 + \frac{kEI}{K_sGA} + \frac{EI\rho}{K_sG}\partial_t{}^2\right)\frac{a^2}{4}\right]w^{(4)} + \left[\left(\rho I\partial_t{}^2 + \frac{kEI}{K_sGA} + \frac{EI\rho}{K_sG}\partial_t{}^2\right) + \left(k + \rho A\partial_t{}^2\right)\frac{a^2}{12} + \left(\frac{k\rho I}{K_sGA}\partial_t{}^2 + \frac{\rho^2 I}{K_sG}\partial_t{}^4\right)\frac{a^2}{3}\right]w^{(2)} - \left[\left(k + \rho A\partial_t{}^2\right) + \frac{k\rho I}{K_sGA}\partial_t{}^2 + \frac{\rho^2 I}{K_sG}\partial_t{}^4\right]w = 0 \quad (94)$$

Supposing a harmonic wave equation in the form of Eq. (11) leads to

$$\left[\frac{\rho^2}{EK_sG}\left(1 + \frac{a^2}{3}k_w{}^2\right)\right]\omega^4 - \left[\left(\frac{\rho}{E} + \frac{\rho}{K_sG}\right)\left(\frac{a^2}{4}\right)k_w{}^4 + \left(\frac{\rho}{E} + \frac{\rho}{K_sG} + \left(\frac{k\rho}{EK_sGA} + \frac{\rho A}{4EI}\right)\frac{a^2}{3}\right)k_w{}^2 + \left(\frac{\rho A}{EI} + \frac{k\rho}{EK_sGA}\right)\right]\omega^2 + \left[\left(\frac{a^2}{6}\right)k_w{}^6 + \left(1 + \frac{ka^2}{4K_sGA}\right)k_w{}^4 + \left(\frac{k}{K_sGA} + \frac{ka^2}{12EI}\right)k_w{}^2 + \frac{k}{EI}\right] = 0 \quad (95)$$

The non-dimensional equation of this approach could be obtained using Eq. (19) with respect to the bending wave velocity definition as follows:

$$\left[\left(\frac{(ak_w)^2}{3} + 1\right)\right]\Omega_b{}^4 - \left[\left(\frac{1}{\mu_s r^{*2}} + \frac{1}{r^{*2}}\right)\frac{(ak_w)^4}{4} + \left(\frac{1}{\mu_s r^{*2}} + \frac{1}{r^{*2}} + \left(k^* + \frac{1}{4\mu_s r^{*4}}\right)\frac{1}{3}\right)(ak_w)^2 + \left(\frac{1}{\mu_s r^{*4}} + k^*\right)\right]\Omega_b{}^2 + \left[\left(\frac{1}{\mu_s r^{*4}}\right)\frac{(ak_w)^6}{6} + \left(\frac{1}{\mu_s r^{*4}} + \frac{k^*}{4r^{*2}}\right)(ak_w)^4 + \left(\frac{k^*}{r^{*2}} + \frac{k^*}{12\mu_s r^{*4}}\right)(ak_w)^2 + \frac{k^*}{\mu_s r^{*4}}\right] = 0 \quad (96)$$

The dimensionless bending frequency results obtained through the Padé polynomial expansions are plotted in Fig. 4 for the two branches. Again, for a numeral example defined in Eq. (73) and

with respect to the equations presented by Eq. (13), (57), (80), (89) and (95), the calculations are done.

(a) (b)

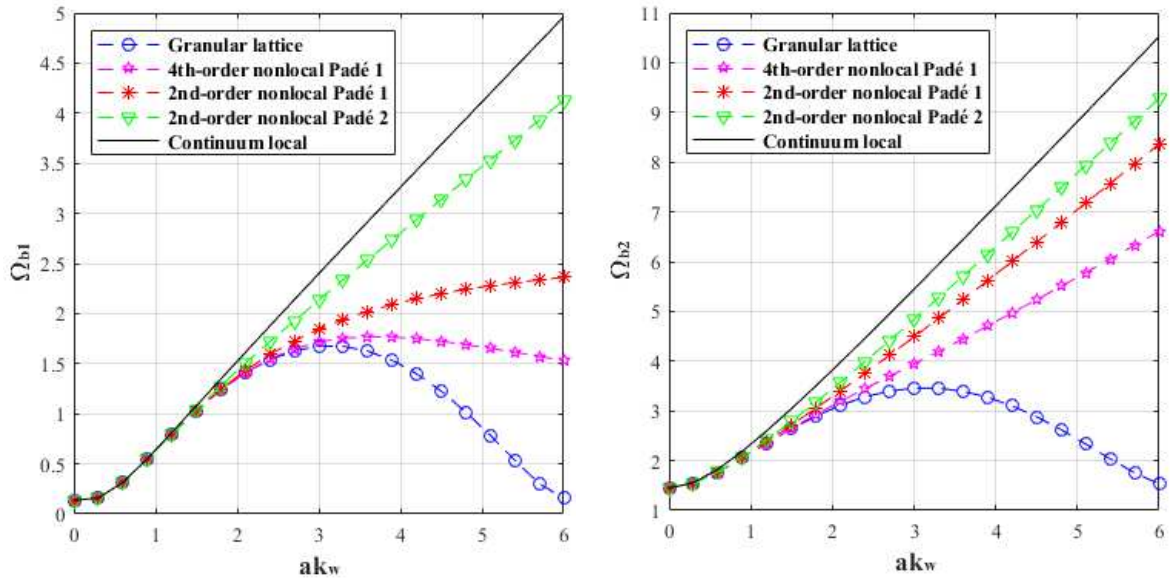

Fig. 4. Dispersive curves for one-dimensional compression wave of (a) first branch and (b)second branch according to bending nondimensional parameter for $\mu_s = 4.28$, $r^* = 0.289$ and $k^* = 0.02$.

4. Discussion

The dispersive results using Eq. (13), (57), (62), (64), (71), (80), (89) and (95) are plotted for shear dimensionless frequency in Fig. 5. There exist two solutions leading to the two branches of the dynamic response of the system each refers to low and high frequencies. The lower branch refers to the acoustic mode and the higher one is the optical mode.

Assuming the mechanical parameters as *E= 200GPa, G= 70GPa,* K_s*= 0.667,* $\rho = 8000kg/m^3$ and *k=50MPa.* For the long-wave limit ($ak_w \rightarrow 0$), the dispersive results obtained from the discrete and continuous model must be equivalent. So, the velocity at the infinite wavelength of the discrete model could

be considered equal to the compression wave velocity of the classical elastic continuum. The divergence of the discrete and continuum frequencies for the wave number increase is obvious. Thus, the inhomogeneous effect by the particle size becomes more prominent or in the other words, the granular models behave more dispersive.

According to the sinusoidal dispersive curve of the exact results, when the curve meets the horizontal axis ($\omega = 0$), it continues periodically. Therefore, it can be concluded that for the exact discrete approach, the responses are always stable. Likewise, the dispersive curves of the Padé approximants could be considered stable as they increase continually from zero without any imaginary part. The unstable harmonic responses appear when the downward branch of the Taylor dispersive curve encounters axis $\omega = 0$.

(a) (b)

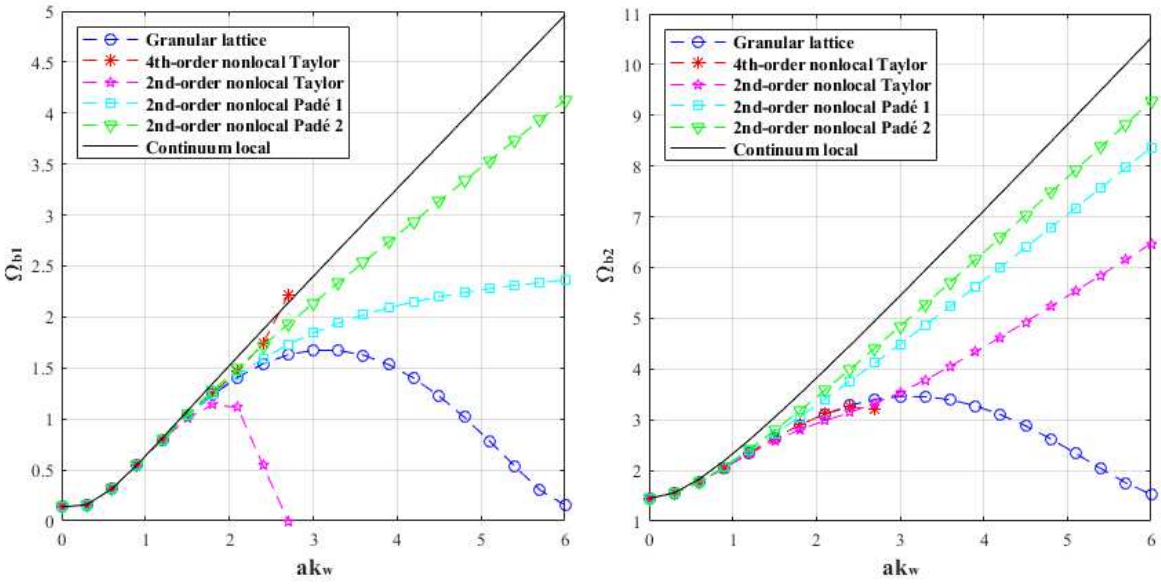

Fig. 5. Dispersive curves for one-dimensional compression wave of (a) first branch or the acoustic mode and (b)second branch or the optical mode according to shear nondimensional parameter- various approaches for $\mu_s = 4.28$, $r^* = 0.289$ and $k^* = 1.03$.

The derivation of $\frac{\partial \omega}{\partial k_w}$ represent the wave propagation speed in the system. The existence of the maximum point in the exact and Taylor dispersive results where $\frac{\partial \omega}{\partial k_w} = 0$, the wave energy can't propagate and it represents a standing wave. The dispersive results for the Taylor approach of the pair order and exact discrete solution show the same behavior in which both proceed into a downward trend after passing from a maximum frequency.

Since all the frequencies are in the limited domain, the transition of only low frequencies is possible and consequently, it can be supposed that the media act as a granular filter. This is in contrast to the Padé results and continuum curve since the dispersive curve increases continuously and so all ranges of frequencies can be transmitted.

Here, parametric studies are carried out in order to figure out how intergranular stiffness contributes to the dispersive behavior of the material. To this aim, the influence of Young modulus on the wave velocity (c_0) and μ_s has been studied in Fig. 6 and Fig. 7. The dispersive curves of the first branch frequency for the granular chain are plotted for different approaches.

(a) (b)

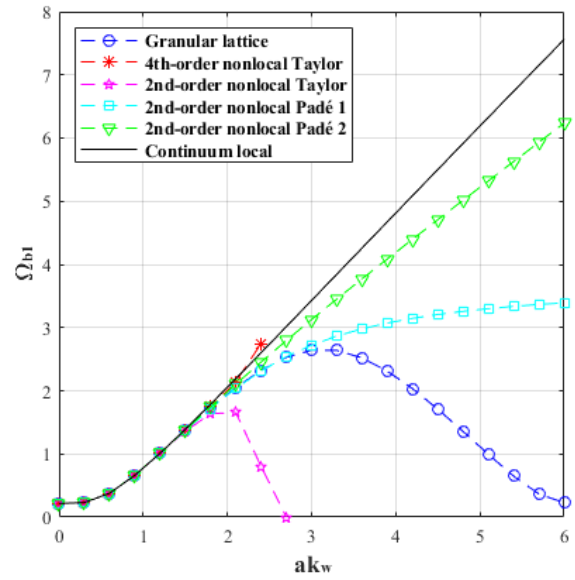

(c)

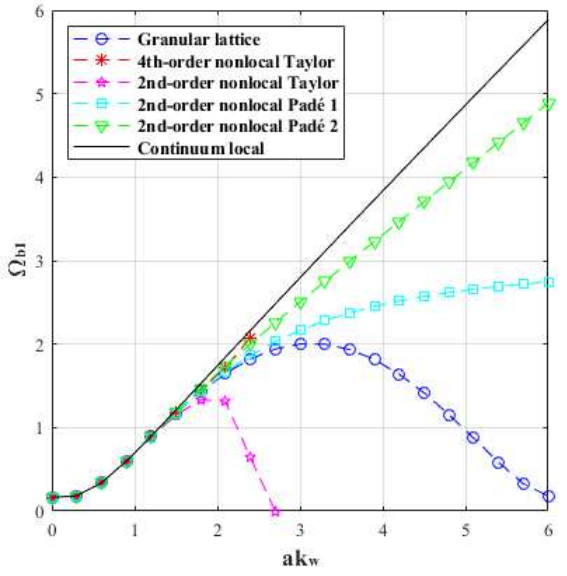

(d)

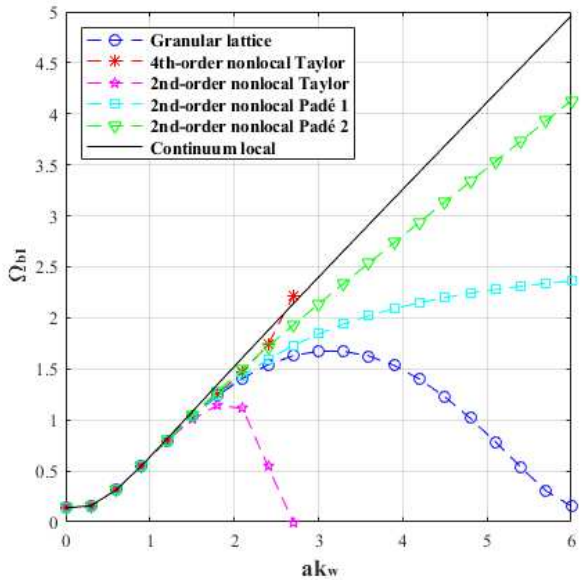

(a)

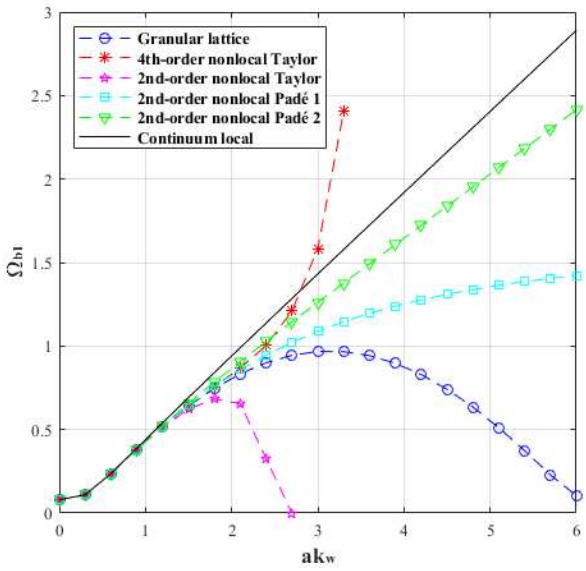

(b)

Fig. 6. Comparison of the first branch of natural frequency for the different values of Young modulus in 1D media: (a) $c_0 = 3162$ m/s^2 and$d$ $\mu_s = 1.71$, (b) $c_0 = 4183$ m/s^2 and $\mu_s = 2.99$, (c) $c_0 = 5000$ m/s^2 and $\mu_s = 4.28$ and (d) $c_0 = 8660$ m/s^2 and $\mu_s = 12.85$ for $r^* = 0.289$ and $k^* = 0$.

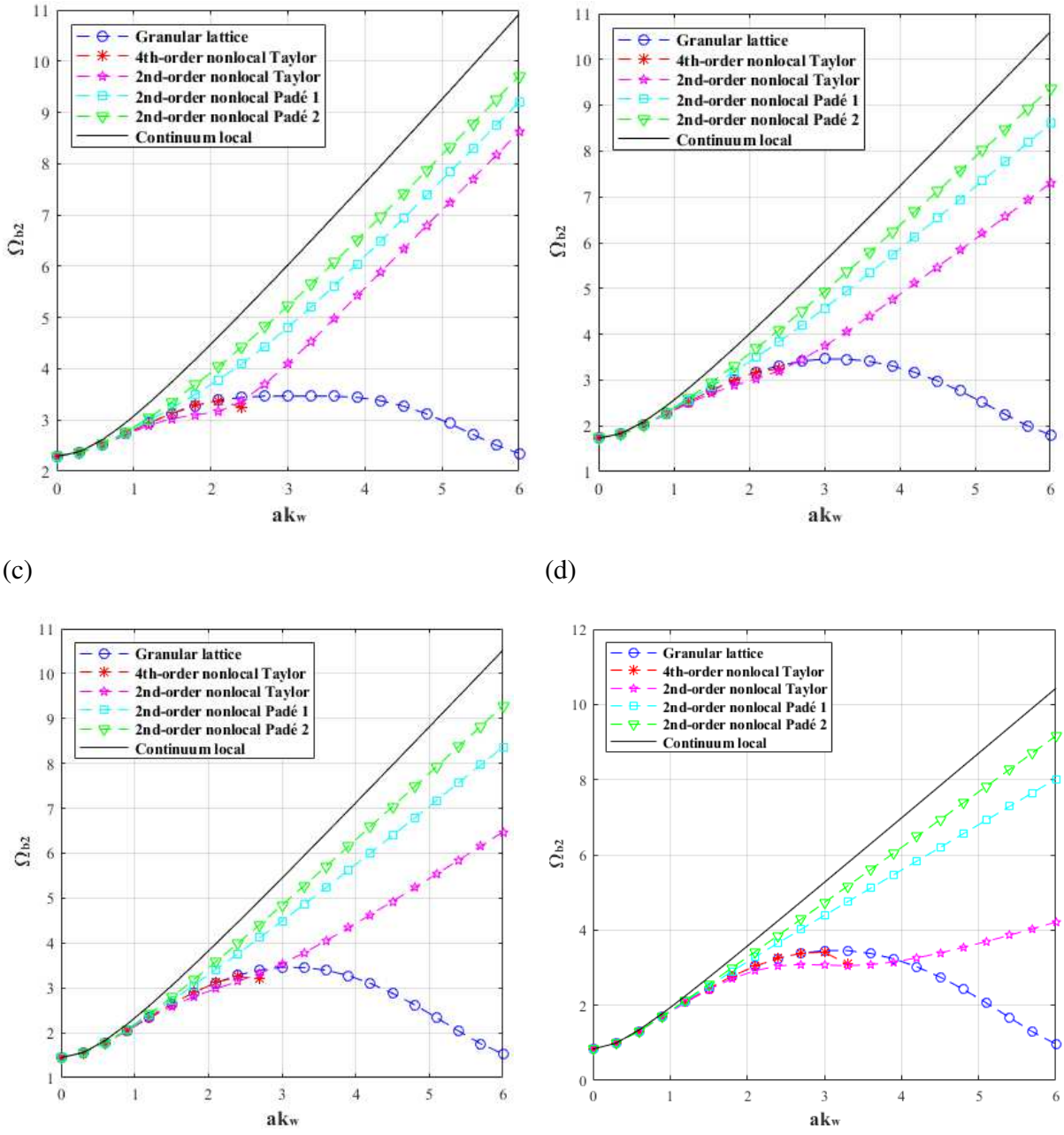

Fig. 7. Comparison of the second branch of natural frequency for the different values of Young modulus in 1D media: (a) $c_0 = 3160\ m/s2$ and$d\ \mu_s = 1.71$, (b) $c_0 = 4183\ m/s2$ and $\mu_s = 2.99$, (c) $c_0 = 5000$ m/s^2 and $\mu_s = 4.28$ and (d) $c_0 = 8660\ m/s2$ and $\mu_s = 12.85$ for $r^* = 0.289$ and $k^* = 0$.

The bending behavior of Carbon Nanotubes (CNTs) could be modeled quite well by Timoshenko beam theory. In this study for short tubes, the short wavelengths or high frequencies are investigated and the results compared by the molecular dynamics results of Wang and Hu [43] a different gradient enrichment of the Timoshenko beam theory for (5,5) and (10,10) armchair CNTs.

In this article, the effective parameters reported as K_s= *0.5,* ρ =$2237kg/m^3$, *k=0MPa, E= 460GPa* and *G= 188.5GPa* for (5,5) CNT and *E= 470GPa* and *G= 195.8GPa* for (10,10) CNT. The cross-section area and the second moment of inertia could be calculated subsequently by $A = 2\pi rt$ and $I = \pi(R^3t + 0.25t^3R)$, where R is the radius of the CNT and t is the wall thickness. According to Domenico and Askes [36] for C-C bond length of $l = 0.142nm$ the closest longitudinal distance between two rings of atoms in an armchair CNT given by $L = \sqrt{3}l$ and R the radius of the CNT would be found by $R = \frac{3nl}{2\pi}$ (for $n = 5, 10$). The thickness of the tube wall is supposed $t = 0.0617nm$ (Vodenitcharova and Zhang [44]).

(a) (b)

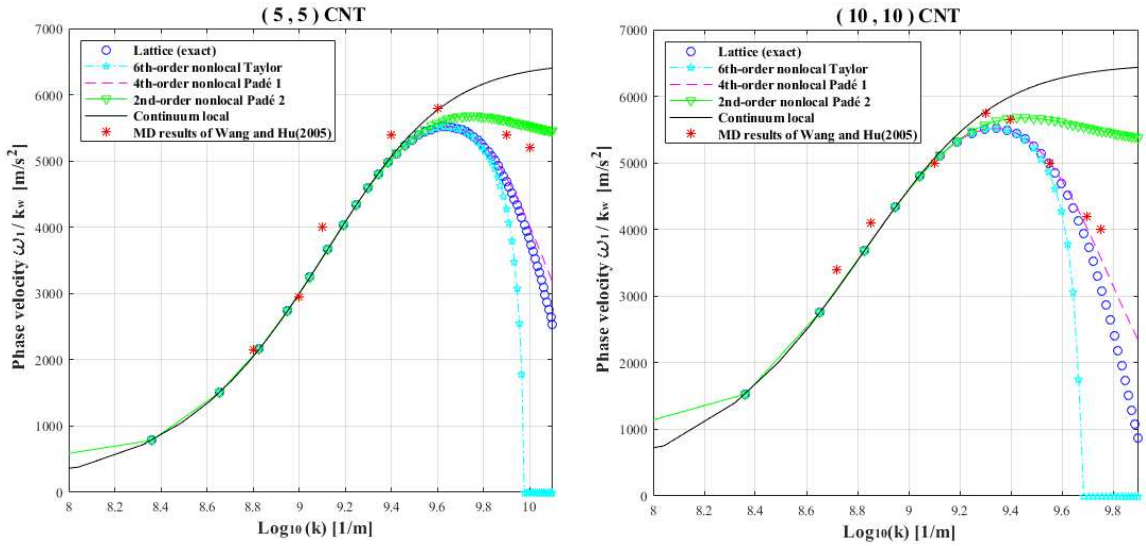

Fig. 8. Comparison of the different approach with the molecular dynamics results of Wang and Hu [43]: (a) (5,5) and (b) (10,10) armchair CNT - various approaches

5. Conclusion

Wave dispersion occurs in granular systems, when the characteristic length scale of the discrete model is of the same order as the wavelength of the waves propagating through the equivalent continuous media. In order to capture this effect, a discrete Cosserat theory has been used to analyze the wave propagation in discrete granular chains. First, the exact dispersive equation of the system has been obtained from the uncoupled equation of motion of the discrete granular chain resting on Winkler foundations. Using the exact resolution of the difference equation of the discrete system, it has been clarified that the two branches of eigenfrequencies exist for the granular model which leads to the ones obtained in the literature, namely by Bresse and Timoshenko for an infinite number of grains. Next, the model has been homogenized using non-local gradient terms by two approaches based on Taylor series and Padé approximations. It has been shown that the dispersion behavior of higher-order continuous models is improved by considering additional gradient enrichments terms, as compared to the initial discrete one. It can be also concluded that, as observed for the dispersion curves of the discrete granular chain, the continuous approximation issued of a Padé approximant is always stable.

References

[1] A. G. Bagdoev, V. I. Erofeev and A. V. Shekoyan, Wave Dynamics of Generalized Continua, Springer-Verlag Berlin Heidelberg, 2016.

[2] I. Vardoulakis, Cosserat Continuum Mechanics With Applications to Granular Media, Springer International Publishing, 2019.

[3] R. D. Mindlin, Micro-structure in linear elasticity, Archive for Rational Mechanics and analysis, 16 (1964) 51-78. https://doi.org/10.1007/BF00248490

[4] E. C. Aifantis, On the role of gradients in the localization of deformation and fracture, Journal of Engineering Science, 30 (10) (1992) 1279-1299.
https://www.sciencedirect.com/science/article/abs/pii/0020722592901413

[5] A. Eringen, On differential equations of nonlocal elasticity and solutions of screw dislocation and surface waves, Journal of Applied Physics, 54 (1983) 4703-4710.
https://aip.scitation.org/doi/10.1063/1.332803

[6] J. Duffy, Stress–strain relations and vibrations of granular medium, Colombia Univ, New York, 1957.

[7] P. J. Digby, The effective elastic moduli of porous granular rock, Journal of Applied Mechanics, 48 (1981) 803-808. https://scinapse.io/papers/1991585306

[8] C. S. Chang, Micromechanical modelling of constitutive relations for granular material, Micromechanics of granular material, (1988) 271-279.
https://www.sciencedirect.com/science/article/pii/B9780444705235500382

[9] H. B. Mühlhaus and I. Vardoulakis, The thickness of shear bands in granular materials, Geotechnique, 37 (3) (1987) 271-283. https://www.icevirtuallibrary.com/doi/10.1680/geot.1987.37.3.271

[10] G. La-Valle and S. Massoumi, A new deformation measure for micropolar plates subjected to in-plane loads, Continuum Mechanics and Thermodynamics, (2021) https://doi.org/10.1007/s00161-021-01055-7

[11] A. S. J. Suiker, C. S. Chang, R. D. Borst and C. Esveld, Surface waves in a stratified half space with enhanced continuum properties, Journal of Applied Mechanics, 18 (1999) 749–768.
https://www.sciencedirect.com/science/article/pii/S0997753899001072

[12] C. S. Chang and L. Ma, Elastic material constants for isotropic granular solids with particle rotation, Journal of Solids Structure, 29 (1992) 1001-1018.
https://www.sciencedirect.com/science/article/abs/pii/002076839290071Z

[13] N. Challamel, J. Lerbet, F. Darve and F. Nicot, Buckling of granular systems with discrete and gradient elasticity Cosserat continua, Annals of Solid Structural Mechanics, 12 (2020)
https://doi.org/10.1007/s12356-020-00065-5

[14] L. M. Schwartz, D. L. Johnson and S. Feng, Vibrational modes in granular materials, Physical Review, 52 (10) (1984) 831-834. https://journals.aps.org/prl/abstract/10.1103/PhysRevLett.52.831

[15] F. Gomez-Silva and R. Zaera, Analysis of low order non-standard continualization methods for enhanced prediction of the dispersive behaviour of a beam lattice, Journal of Mechanical Science, 196 (2021) https://www.sciencedirect.com/science/article/abs/pii/S002074032100031X

[16] E. Pasternak and H. B. Mühlhaus, Generalized homogenization procedures for granular materials, Journal of Engineering Mathematics, 51 (1) (2005) 199-229. https://doi.org/10.1007/s10665-004-3950-z

[17] H. Pichard et al., Localized transversal-rotational modes in linear chains of equal masses, Physical Review, 89 (2014) 10.1103/PhysRevE.89.013201

[18] A. A. Vasiliev, A. E. Miroshnichenko and M. Ruzzene, A discrete model and analysis of one-dimensional deformations in a structural interface with micro-rotations, mechanics Research Communications, 37 (2) (2010) 225-229.
https://www.sciencedirect.com/science/article/abs/pii/S0093641309001669

[19] S. Massoumi et al., Static bending of granular beam: Exact discrete and nonlocal solutions, submitted for publication, Manuscript submitted for publication in Meccanica, (2021)

[20] Y. Starosvetsky, K. R. Jayaprakash and A.F. Vakakis, J. Appl. Mech. 79, 011001 (2012). Scattering of solitary waves and excitation of transient breathers in granular media by light intruders and no precompression, Journal of Applied Mathematics, 79 (2012) 11001-11013.
https://asmedigitalcollection.asme.org/appliedmechanics/article-abstract/79/1/011001/475144/Scattering-of-Solitary-Waves-and-Excitation-of?redirectedFrom=fulltext

[21] V. F. Nesterenko, Propagation of nonlinear compression pulses in granular media, Journal of Applied Mechanics and Technical Physics, 24 (1984) 733-743.
https://link.springer.com/article/10.1007/BF00905892

[22] E. B. Herbold et al., Pulse propagation in a linear and nonlinear diatomic periodic chain: effects of acoustic frequency band-gap, Acta Mechanica, 205 (2009) 85-103.
https://link.springer.com/article/10.1007/s00707-009-0163-6

[23] S. Massoumi, N. Challamel and J. Lerbet, Exact solutions for the vibration of finite granular beam using discrete and gradient elasticity Cosserat models, Journal of Sound and Vibration, 494 (2021) 115839. https://doi.org/10.1016/j.jsv.2020.115839

[24] J. A. C. Bresse, Cours de mécanique appliquée – Résistance des matériaux et stabilité des constructions Gautier-Villars, Paris, 1859.

[25] S. P. Timoshenko, On the correction for shear of the differential equation for transverse vibrations of prismatic bars, Philosophical Magazine, 41 (1921) 744-746.

[26] S. P. Timoshenko, On the transverse vibration of bars with uniform cross-section, Philosophical Magazine, 43 (1922) 125-131.

[27] N. Challamel and I. Elishakoff, A brief history of first-order shear-deformable beam and plate models, mechanics Research Communications, 102 (103389) (2019) 1-8. https://www.sciencedirect.com/science/article/abs/pii/S0093641319302289

[28] A. Misra and N. Nejadsadeghi, Longitudinal and transverse elastic waves in {1D} granular materials modeled as micromorphic continua, Wave Motion, 90 (2019) 175-195. https://doi.org/10.1016/j.wavemoti.2019.05.005

[29] A. Misra and P. Poorsolhjouy, Elastic behavior of 2D grain packing modeled as micromorphic media based on granular micromechanics, Journal of Engineering Mechanics, 143 (1) (2016) C4016005.

[30] T. M. Wang and J. E. Stephens, Natural frequencies of Timoshenko beams on Pasternak foundations, Journal of Sound and Vibration, 51 (2) (1977) 149-155. https://www.sciencedirect.com/science/article/abs/pii/S0022460X77800291

[31] F. Y. Cheng and C. P. Pantelides, Dynamic Timoshenko beam-columns on elastic media, Journal of Structure Engineering, 114 (1988) 1524-1550. https://ascelibrary.org/doi/10.1061/%28ASCE%290733-9445%281988%29114%3A7%281524%29

[32] A. I. Manevich, Dynamics of Timoshenko beam on linear and nonlinear foundation: phase relations, significance of the second spectrum, stability, Journal of Sound and Vibration, 344 (2015) 209-220. https://www.sciencedirect.com/science/article/abs/pii/S0022460X15000735

[33] E. Winkler, Die Lehre von der Elasticitaet und Festigkeit, Prague, Dominicus, (1867)

[34] A. D. Myshkis, Mixed functional differential equations, J. Mathematical Sciences, 129 (5) (2005) 4111-4226.

[35] W. H. Duan, N. Challamel, C. M. Wang and Z. Ding, Development of analytical vibration solutions for microstructured beam model to calibrate length scale coefficient in nonlocal Timoshenko beams, Journal of Applied Physics, 114 (2013) 104312-104323. https://doi.org/10.1063/1.4820565

[36] D. D. Domenico and H. Askes, Nano scale wave dispersion beyond the First Brillouin Zone simulated with inertia gradiant continua, Journal of Applied Physics, 124 (2018) https://aip.scitation.org/doi/10.1063/1.5045838

[37] P. Lu, H. P. Lee and C. Lu, Dynamic properties of flexural beams using a nonlocal elasticity model, Journal of Applied Physics, 99 (2006) 073510-073519. https://www.semanticscholar.org/paper/Dynamic-properties-of-flexural-beams-using-a-model-Lu-Lee/b164e6fb5c0d2a1b0e8a725a9b78c7870ba6721d

[38] N. Challamel, C. M. Wang and I. Elishakoff, Discrete systems behave as nonlocal structural elements: Bending, buckling and vibration analysis, European Journal of Mechanics A/Solids, 44 (2014) 125-135. https://www.sciencedirect.com/science/article/abs/pii/S0997753813001204

[39] M. G. Salvadori, Numerical computation of buckling loads by finite differences, ASCE, 116 (1951) 590-624. https://www.semanticscholar.org/paper/Closure-of-%22Numerical-Computation-of-Buckling-Loads-Salvadori/ffdb1fa7e0721241a49968b54e74fae5ed518eb1

[40] M. D. Kruskal and N. J. Zabusky, Stroboscopic perturbation for treating a class of nonlinear wave equations, Journal of Mathematical Physics, 5 (1964) 231-244. https://aip.scitation.org/doi/10.1063/1.1704113

[41] A. Bacigalupo and C. Gambarotta, Generalized micropolar continualization of 1D beam lattices, Journal of Mechanic Science, 155 (2019) 554-570. https://www.semanticscholar.org/paper/Generalized-micropolar-continualization-of-1D-beam-Bacigalupo-Gambarotta/cdfa099a77c74e0b898f3c4e8c7f9d763a8f0986

[42] A. Bacigalupo and L. Gambarotta, Identification of non-local continua for lattice-like materials, Journal of Engineering Science, 159 (2021) https://www.sciencedirect.com/science/article/abs/pii/S0020722520302172?via%3Dihub

[43] L. Wang and H. Hu, Flexural wave propagation in single-walled carbon nanotubes, Physical Review B, 71 (195412) (2005) https://journals.aps.org/prb/abstract/10.1103/PhysRevB.71.195412

[44] T. Vodenitcharova and L. C. Zhang, Effective wall thickness of a single-walled carbon nanotube, Physical Review B, 68 (165401) (2003) https://journals.aps.org/prb/abstract/10.1103/PhysRevB.68.165401